

### Supporting Information

Effects of Crosslink Density and Plasticizer on Thermorheological Properties of Dissociative Guanidine-based Covalent Adaptable Networks

Adelle L. Koenig,<sup>1</sup> Kelsey M. Allis,<sup>2</sup> John S. Lehr,<sup>2</sup> Michael B. Larsen<sup>1\*</sup>

\*Corresponding author: mike.larsen@wwu.edu

<sup>1</sup>Department of Chemistry, Western Washington University, Bellingham, WA, USA 98225

<sup>2</sup>Department of Engineering and Design, Western Washington University, Bellingham, WA, USA 98225

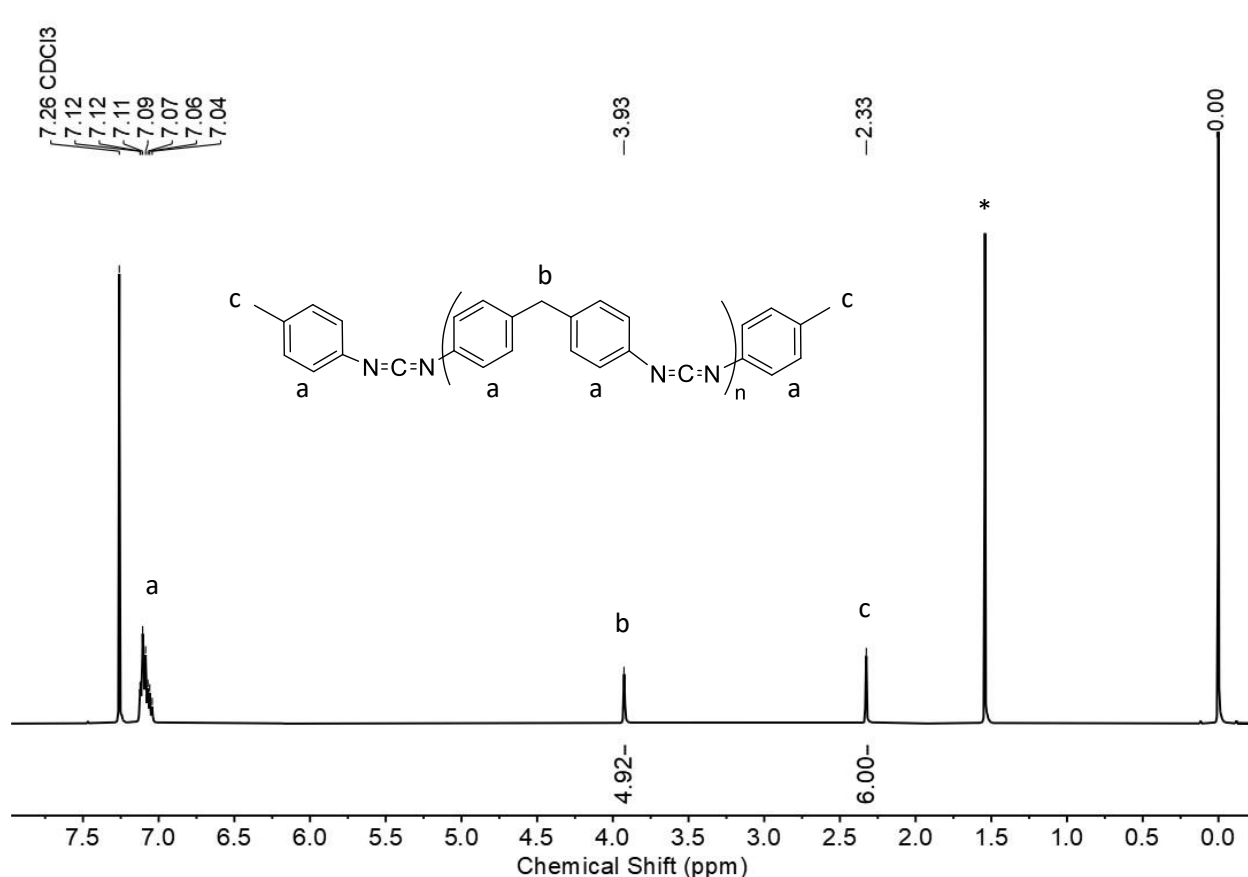


**Figure S1.** <sup>1</sup>H NMR spectrum (500 MHz, CDCl<sub>3</sub>) of multifunctional carbodiimide oligomer. \*H<sub>2</sub>O from CDCl<sub>3</sub>. Degree of polymerization (*n*) was calculated via endgroup analysis by integration of the peak at 2.33 ppm to 6.00 and division by 2 of the resultant integration of the peak at 3.93 ppm.

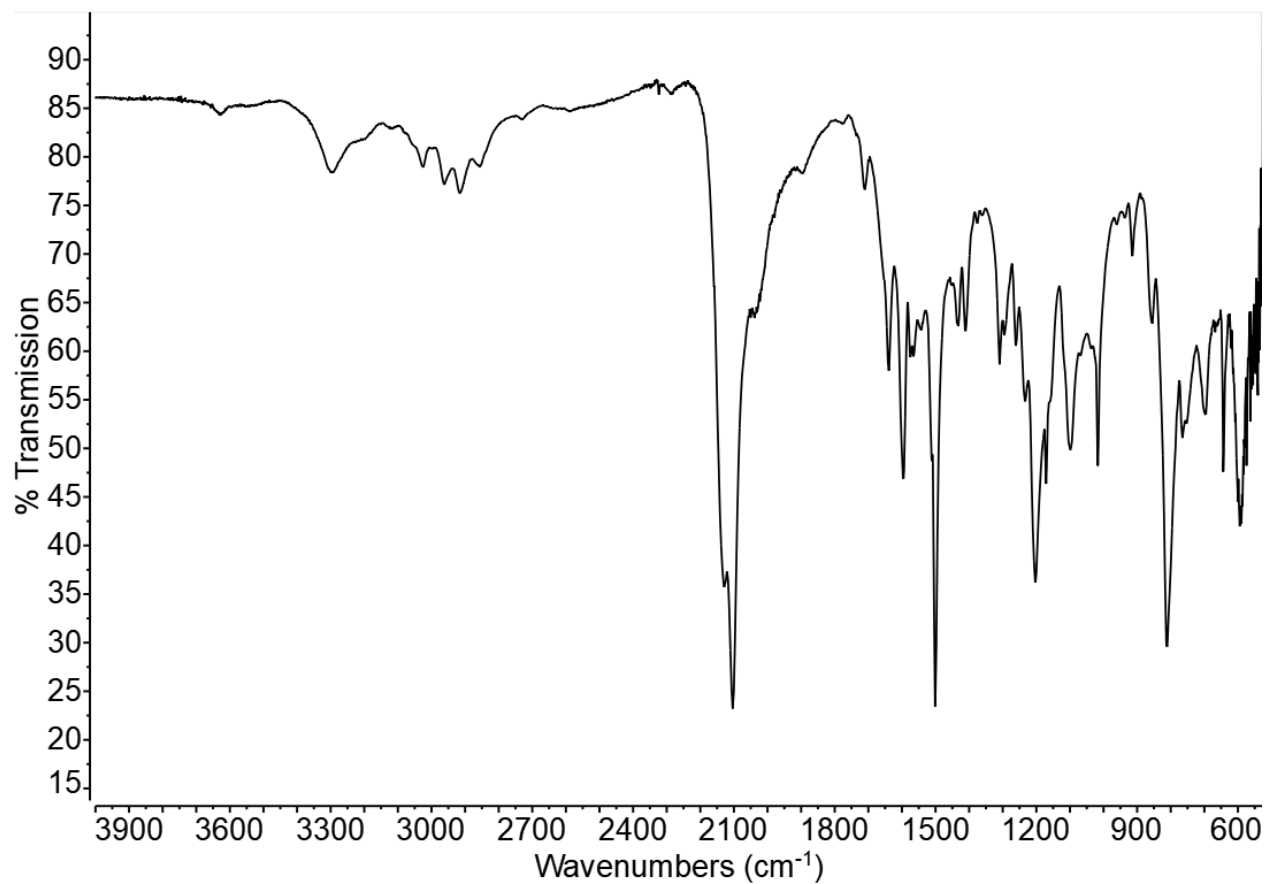


**Figure S2.** ATR FT-IR spectrum of multifunctional carbodiimide oligomer.

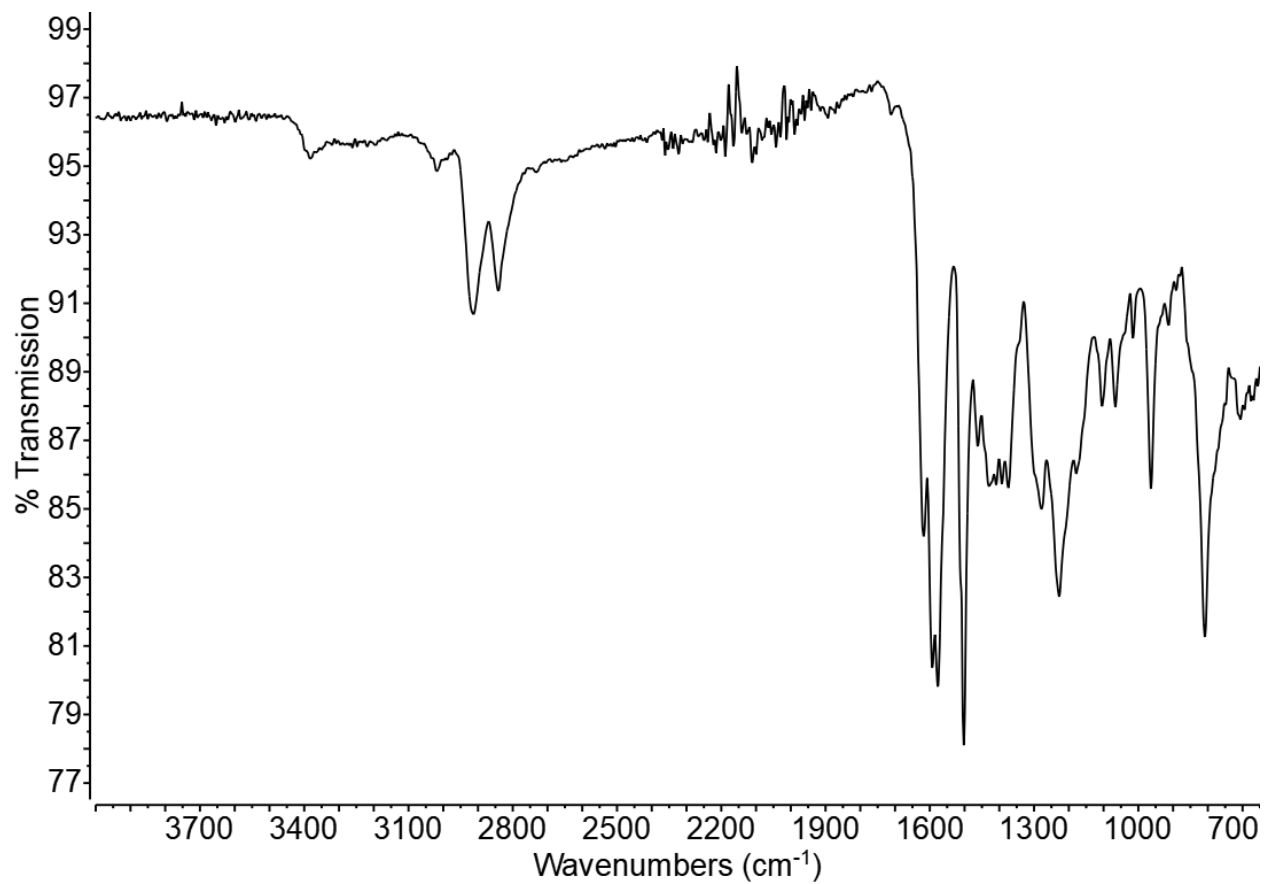


**Figure S3.** ATR FT-IR spectrum of CAN A<sub>0</sub>.

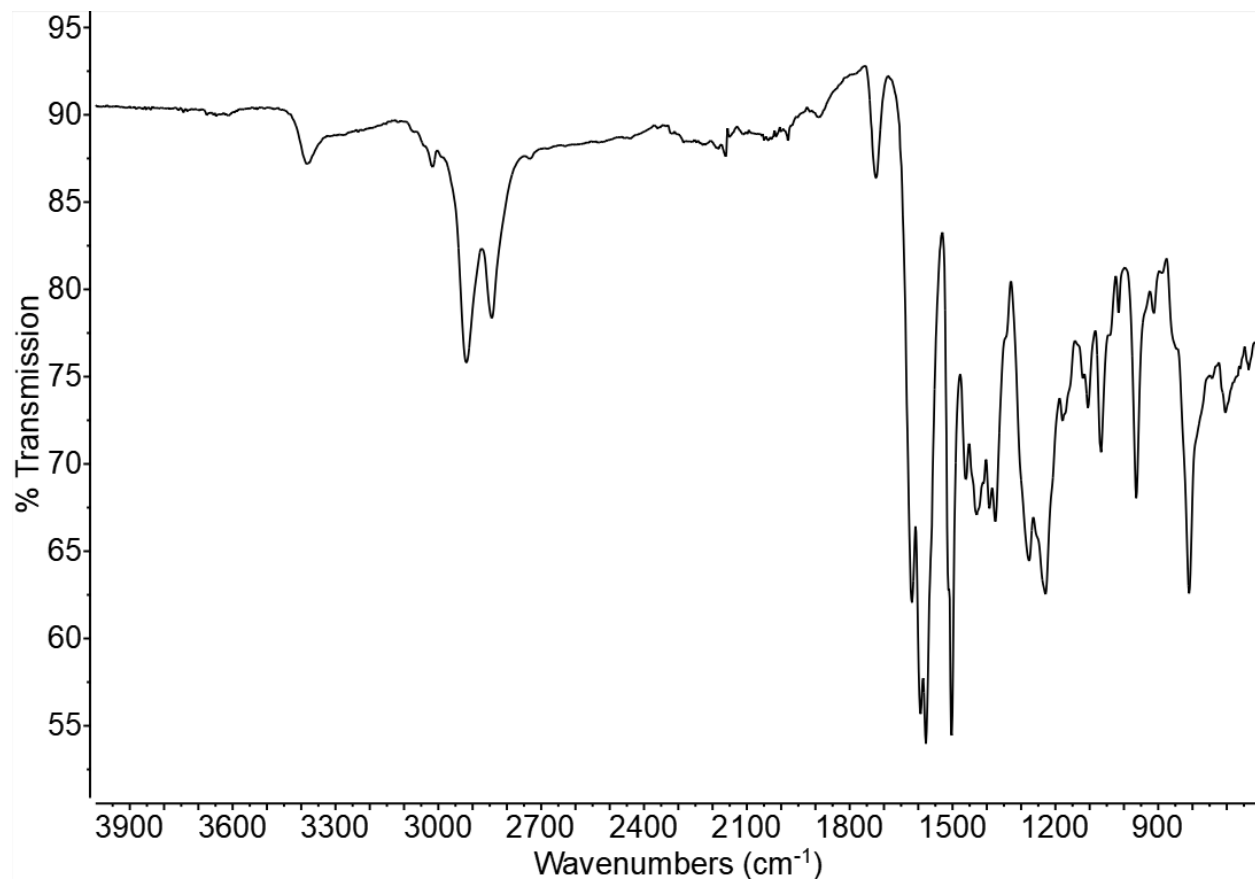


**Figure S4.** ATR FT-IR spectrum of CAN A<sub>5</sub>.

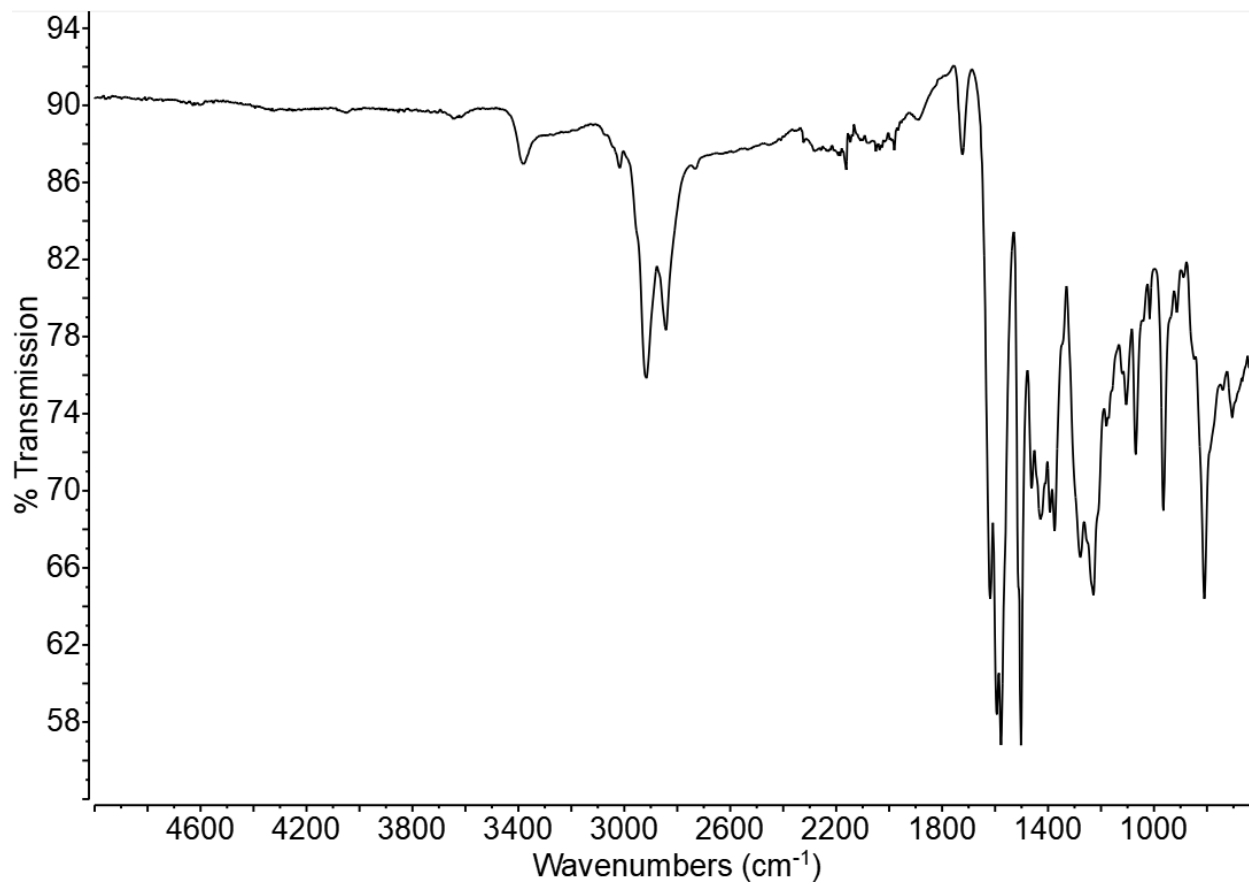


**Figure S5.** ATR FT-IR spectrum of CAN B<sub>5</sub>.

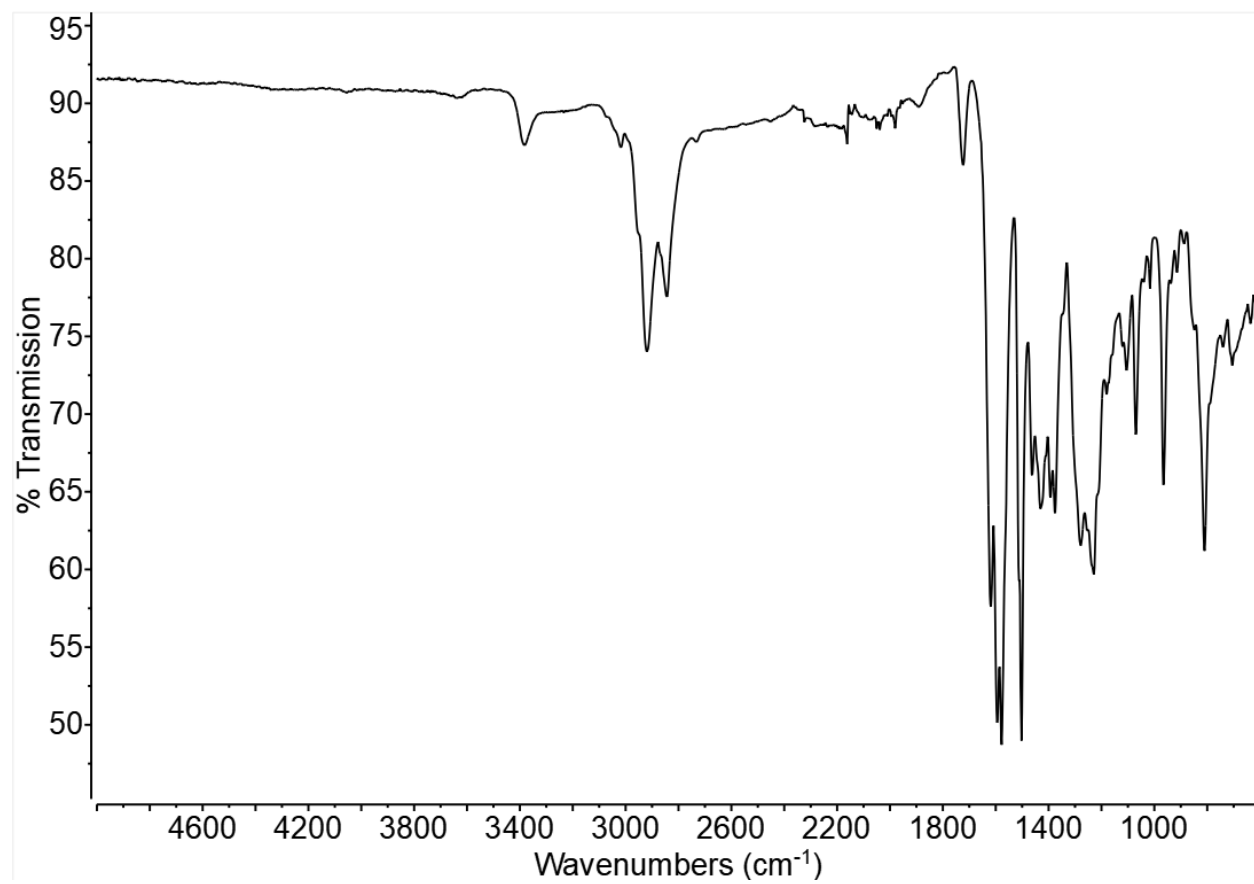


**Figure S6.** ATR FT-IR spectrum of CAN C<sub>5</sub>.

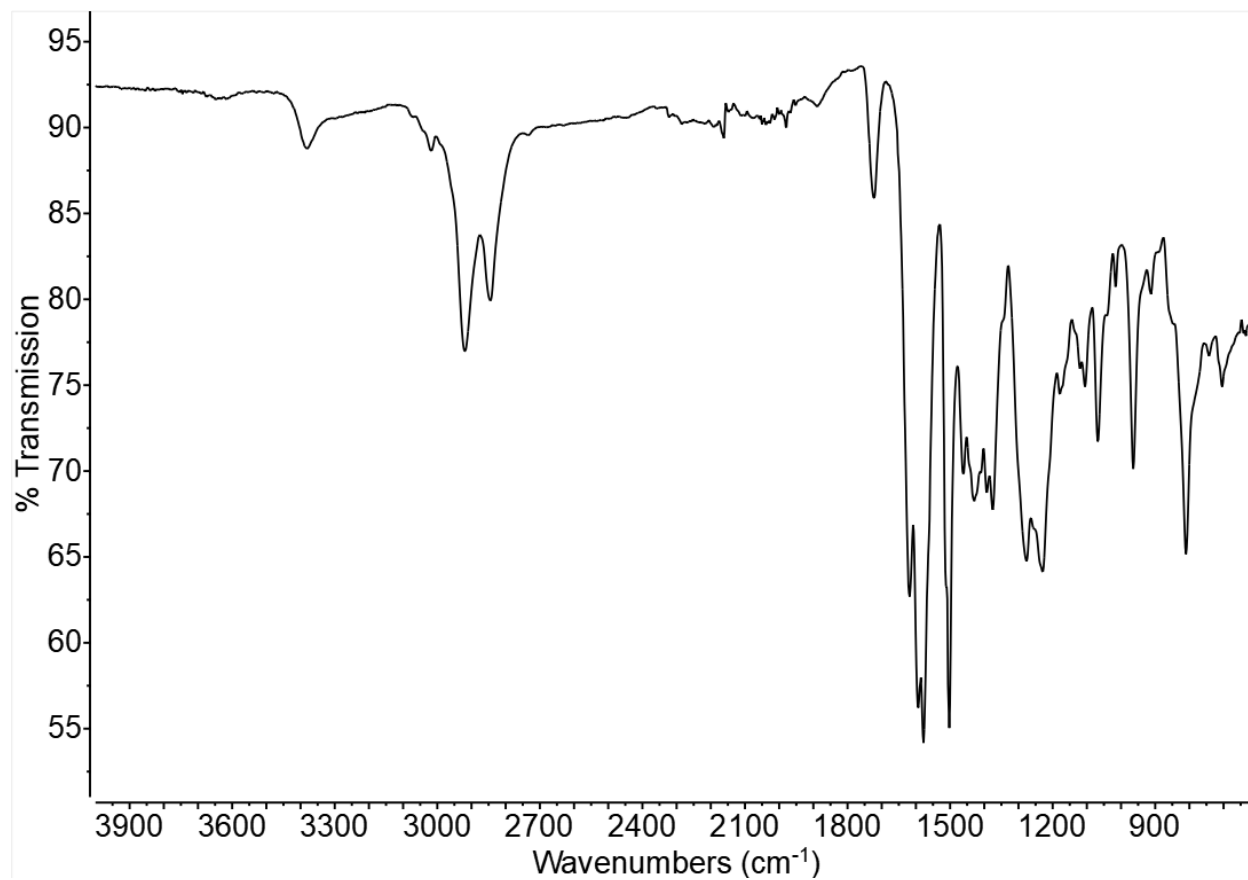


**Figure S7.** ATR FT-IR spectrum of CAN A<sub>10</sub>.

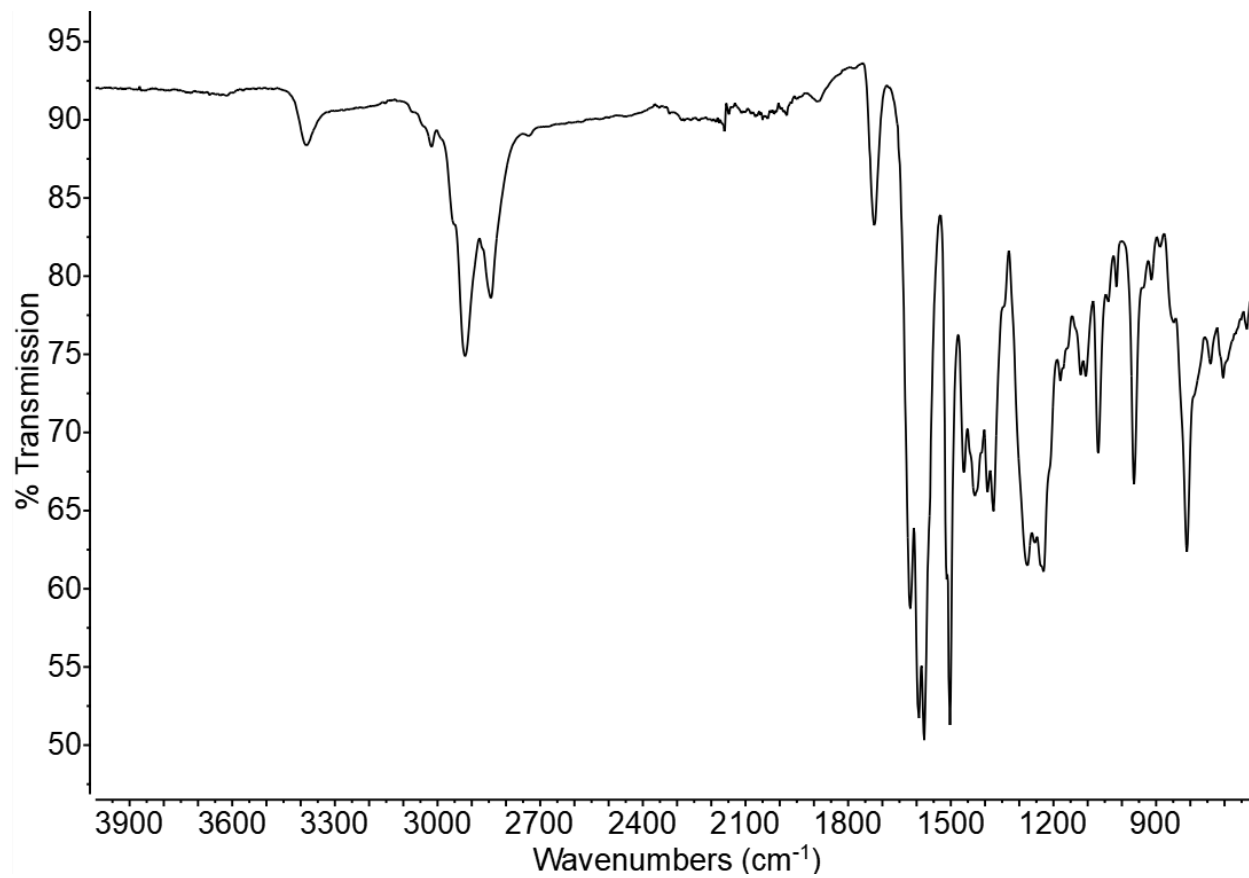


**Figure S8.** ATR FT-IR spectrum of CAN B<sub>10</sub>.



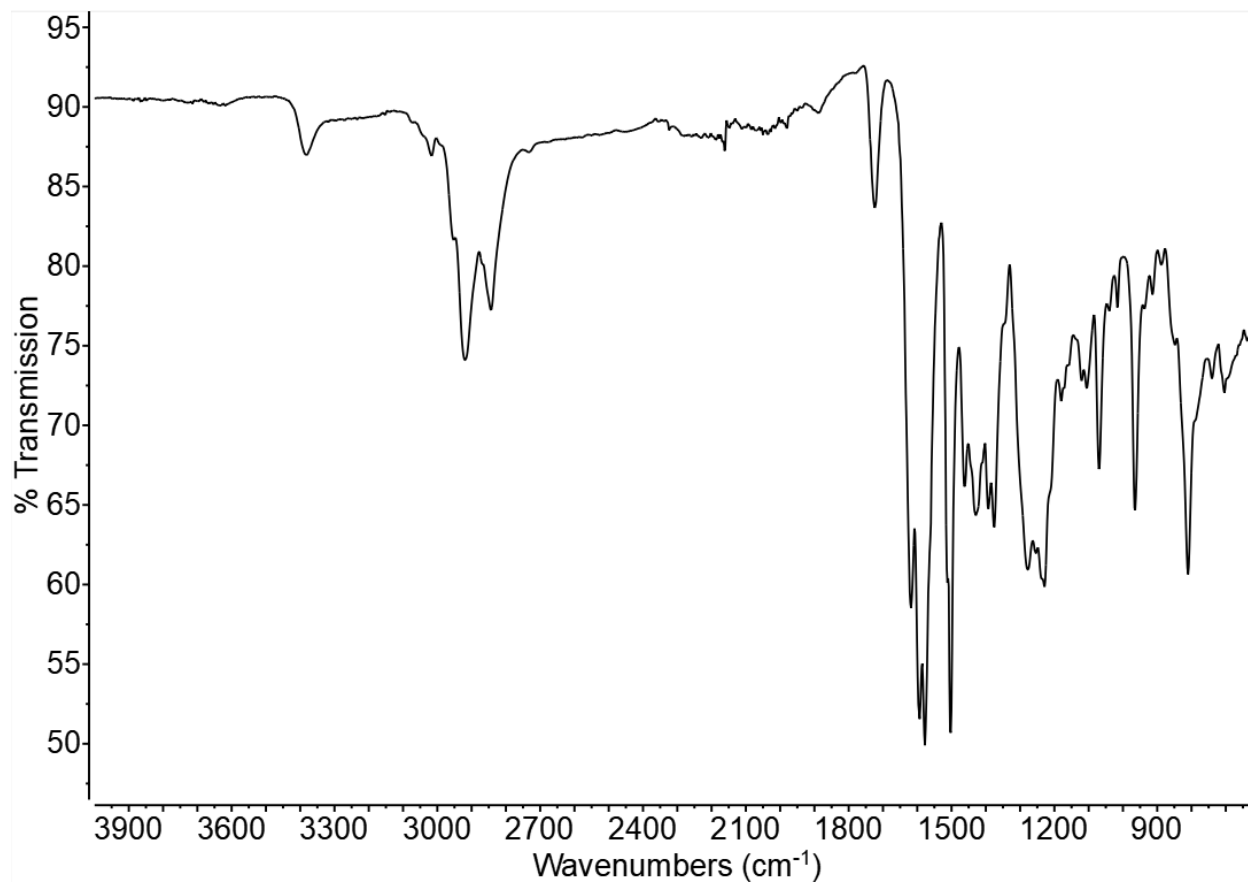


**Figure S9.** ATR FT-IR spectrum of CAN C<sub>10</sub>.

**Table S1.** Mean and standard error of gel fractions for all CAN compositions.

| <b>CAN Composition</b> | <b>Gel Fraction</b>      |
|------------------------|--------------------------|
| CAN A <sub>0</sub>     | 99.3%                    |
| CAN A <sub>5</sub>     | 94.0 ± 3.0% <sup>a</sup> |
| CAN A <sub>10</sub>    | 88.8 ± 0.8% <sup>b</sup> |
| CAN B <sub>5</sub>     | 88.9 ± 1.2% <sup>a</sup> |
| CAN B <sub>10</sub>    | 85.0 ± 1.3% <sup>b</sup> |
| CAN C <sub>5</sub>     | 74.2 ± 2.3% <sup>a</sup> |
| CAN C <sub>10</sub>    | 77.3 ± 6.7% <sup>b</sup> |

<sup>a</sup>Data from three individual samples. <sup>b</sup>Data from two individual samples.

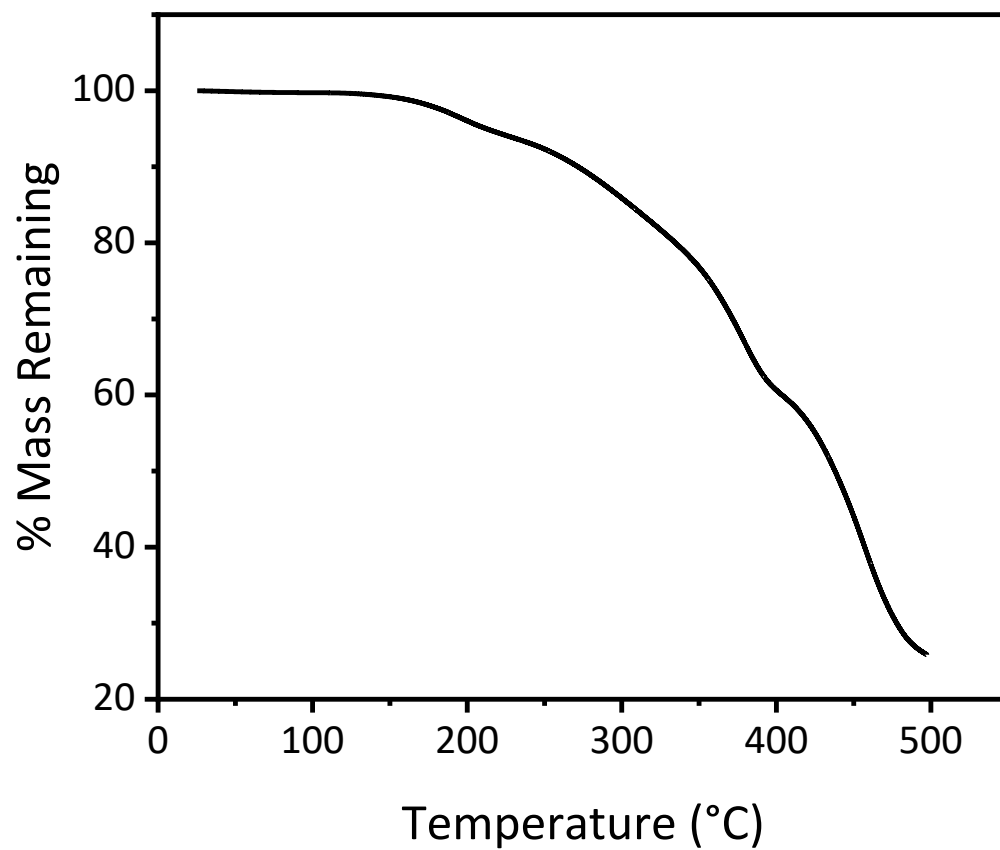


**Figure S10.** TGA thermogram of CAN A<sub>0</sub> (10 °C/min, N<sub>2</sub> atmosphere).  $T_{d,5\%} = 212$  °C.

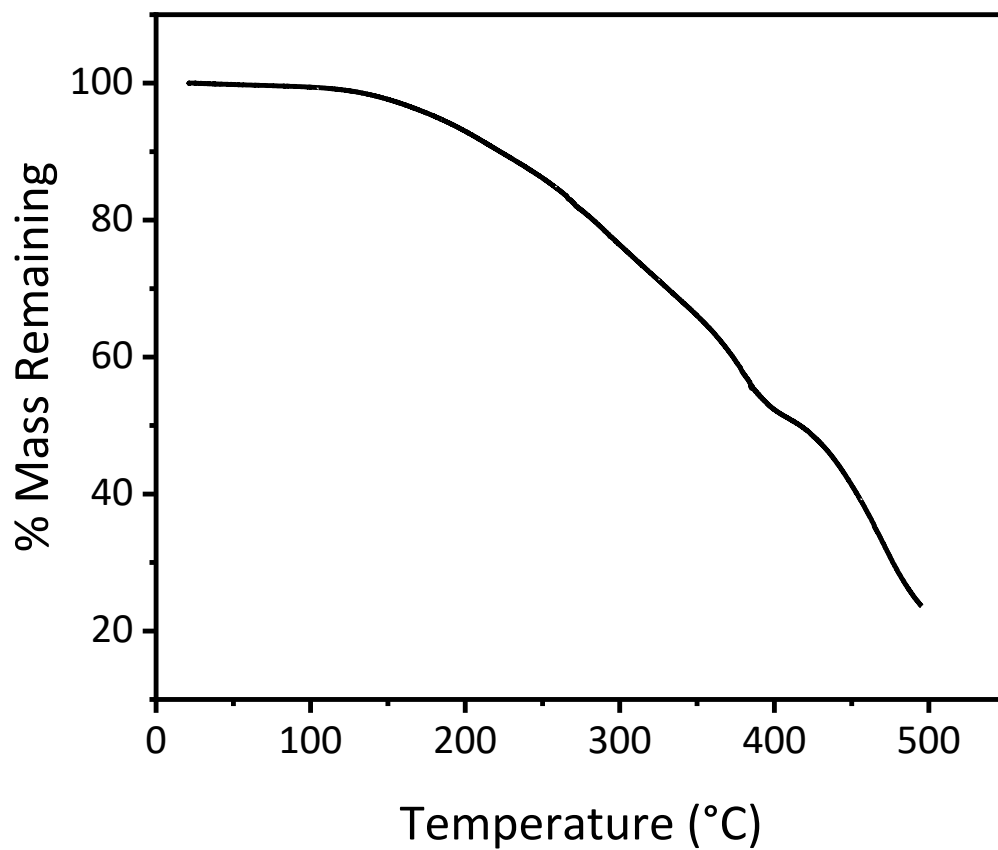


**Figure S11.** TGA thermogram of CAN A<sub>5</sub> (10 °C/min, N<sub>2</sub> atmosphere).  $T_{d,5\%} = 183$  °C.

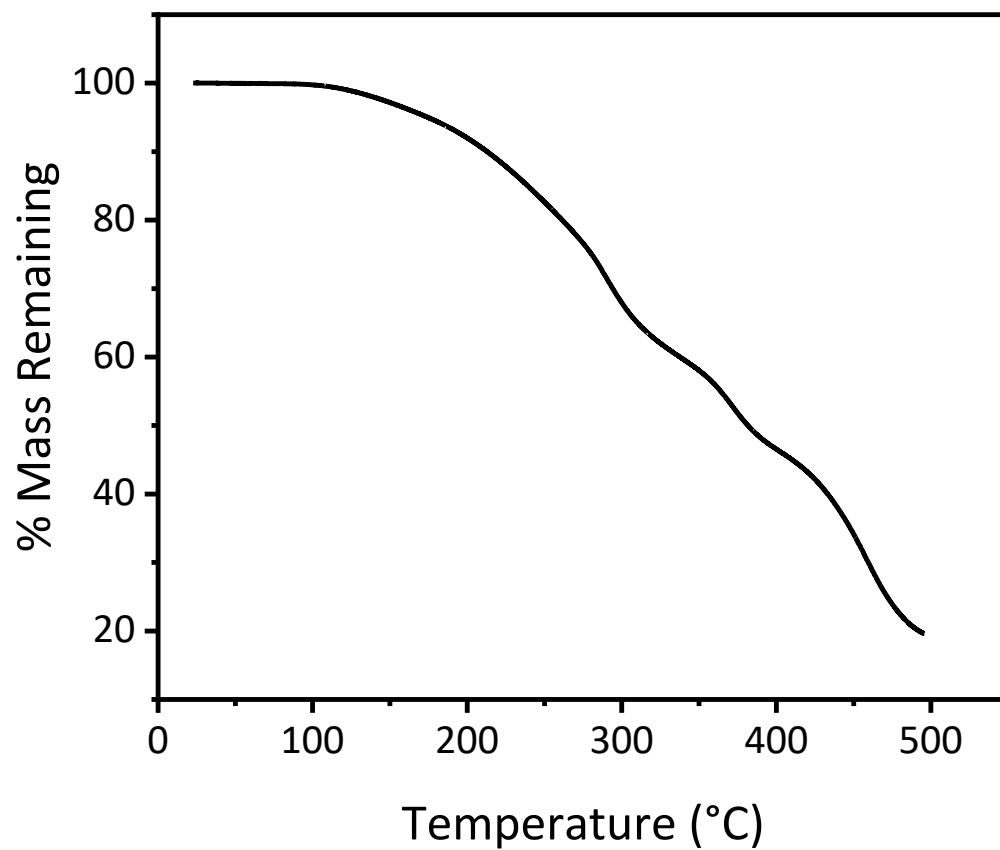


**Figure S12.** TGA thermogram of CAN B<sub>5</sub> (10 °C/min, N<sub>2</sub> atmosphere).  $T_{d,5\%} = 173$  °C.

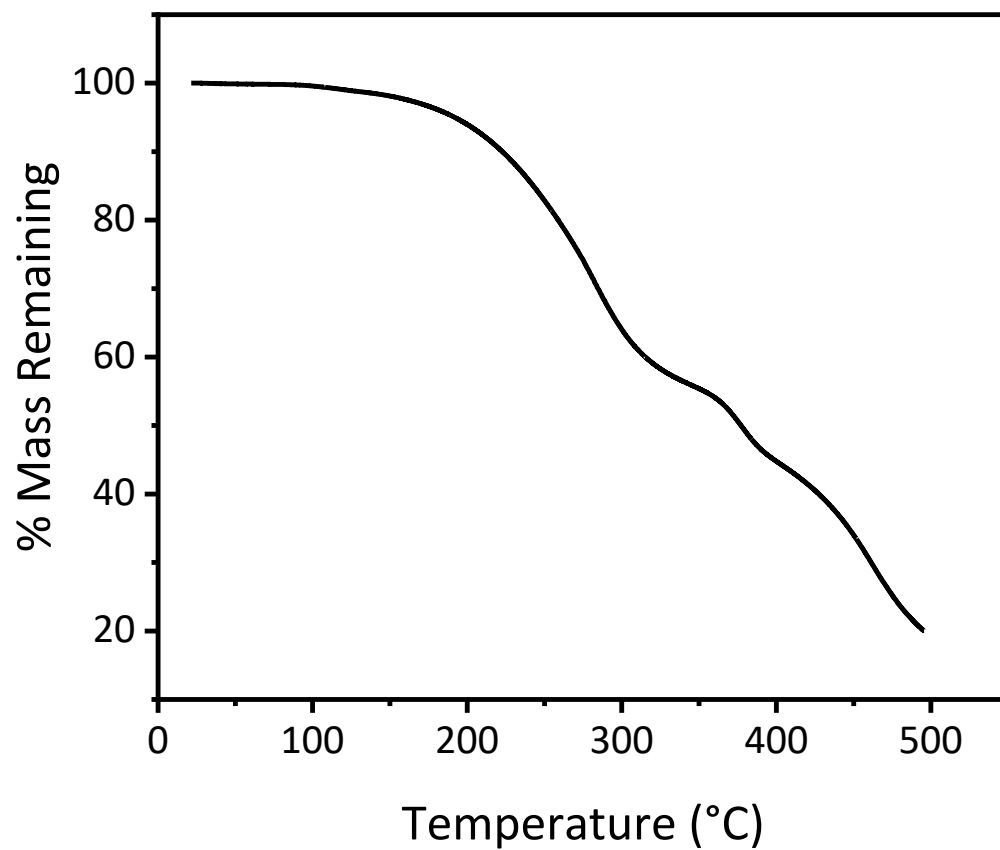


**Figure S13.** TGA thermogram of CAN C<sub>5</sub> (10 °C/min, N<sub>2</sub> atmosphere).  $T_{d,5\%} = 191$  °C.

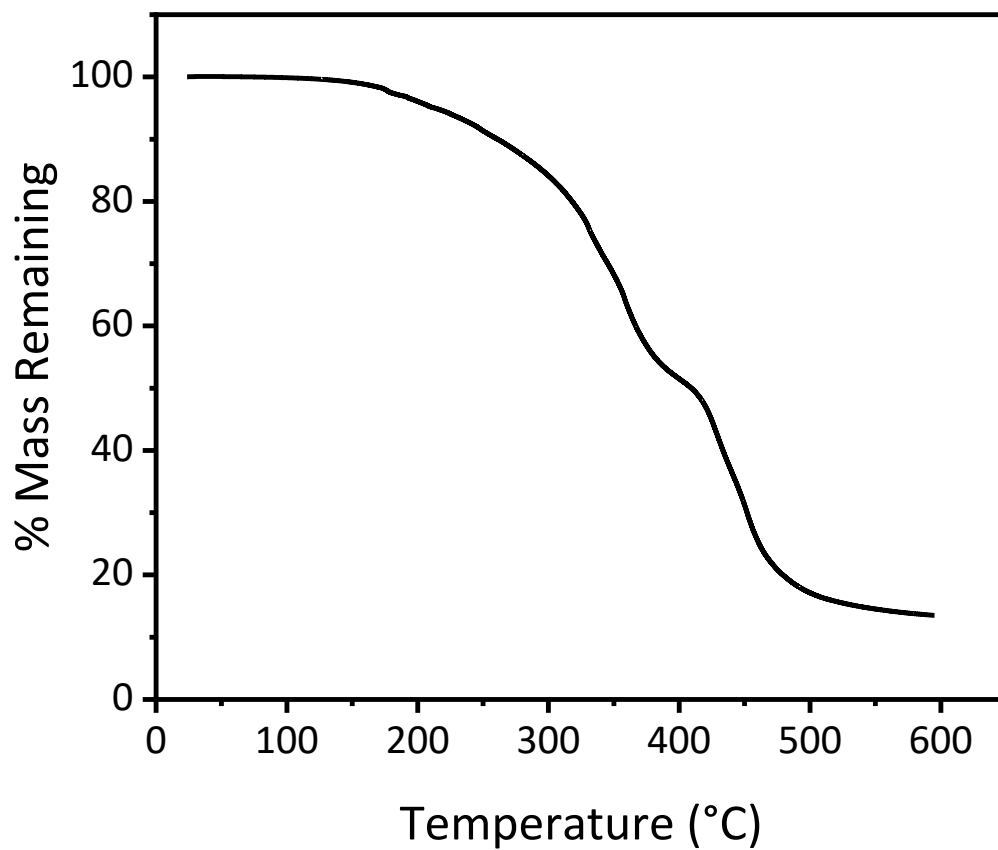


**Figure S14.** TGA thermogram of CAN A<sub>10</sub> (10 °C/min, N<sub>2</sub> atmosphere).  $T_{d,5\%} = 212$  °C.

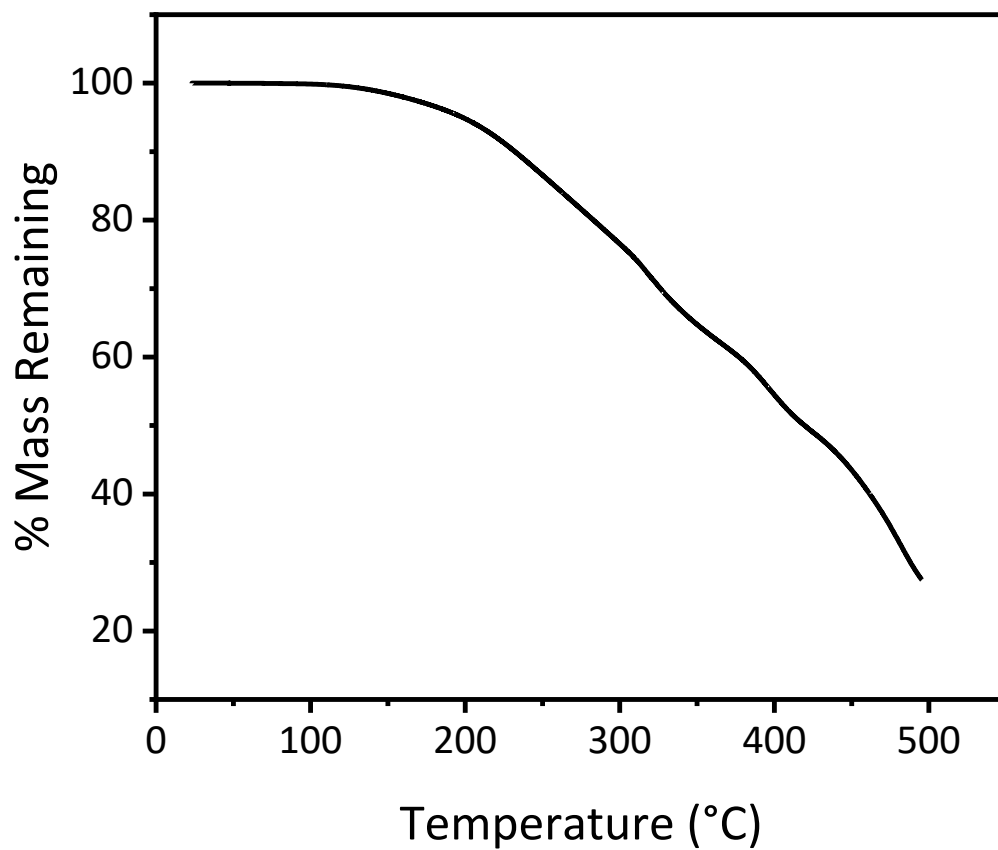


**Figure S15.** TGA thermogram of CAN B<sub>10</sub> (10 °C/min, N<sub>2</sub> atmosphere).  $T_{d,5\%} = 198$  °C.

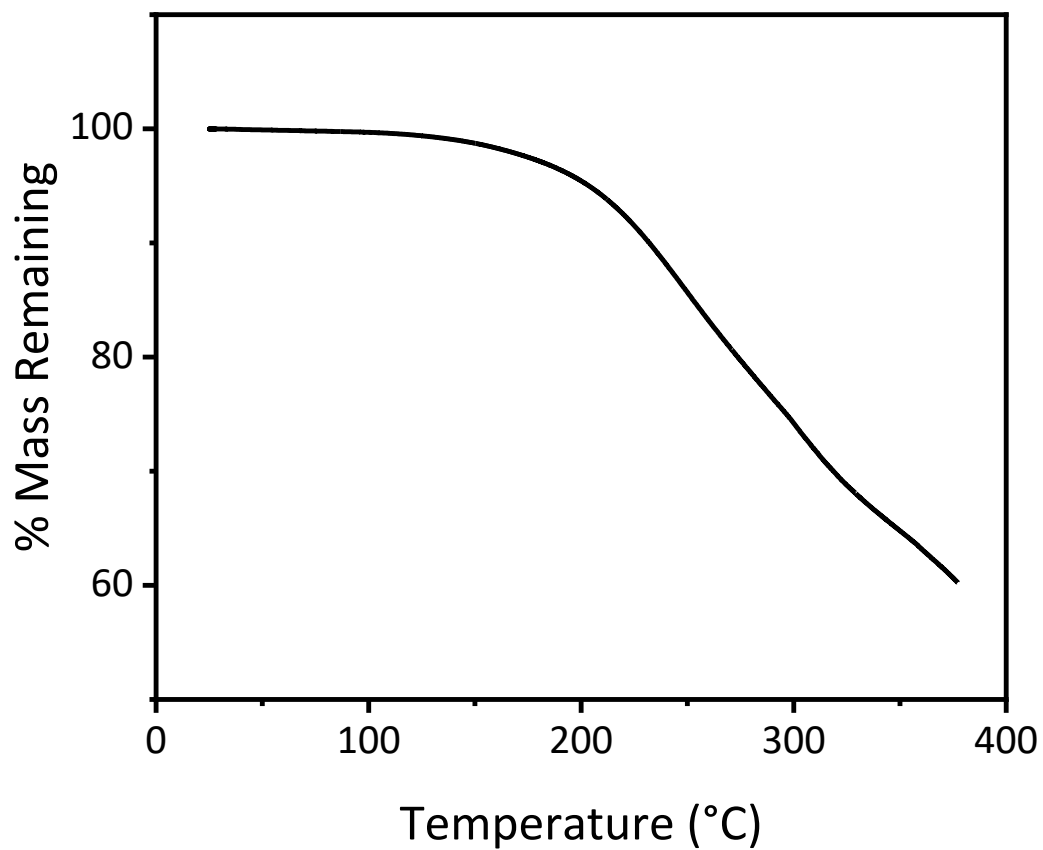


**Figure S16.** TGA thermogram of CAN C<sub>10</sub> (10 °C/min, N<sub>2</sub> atmosphere).  $T_{d,5\%} = 204$  °C.



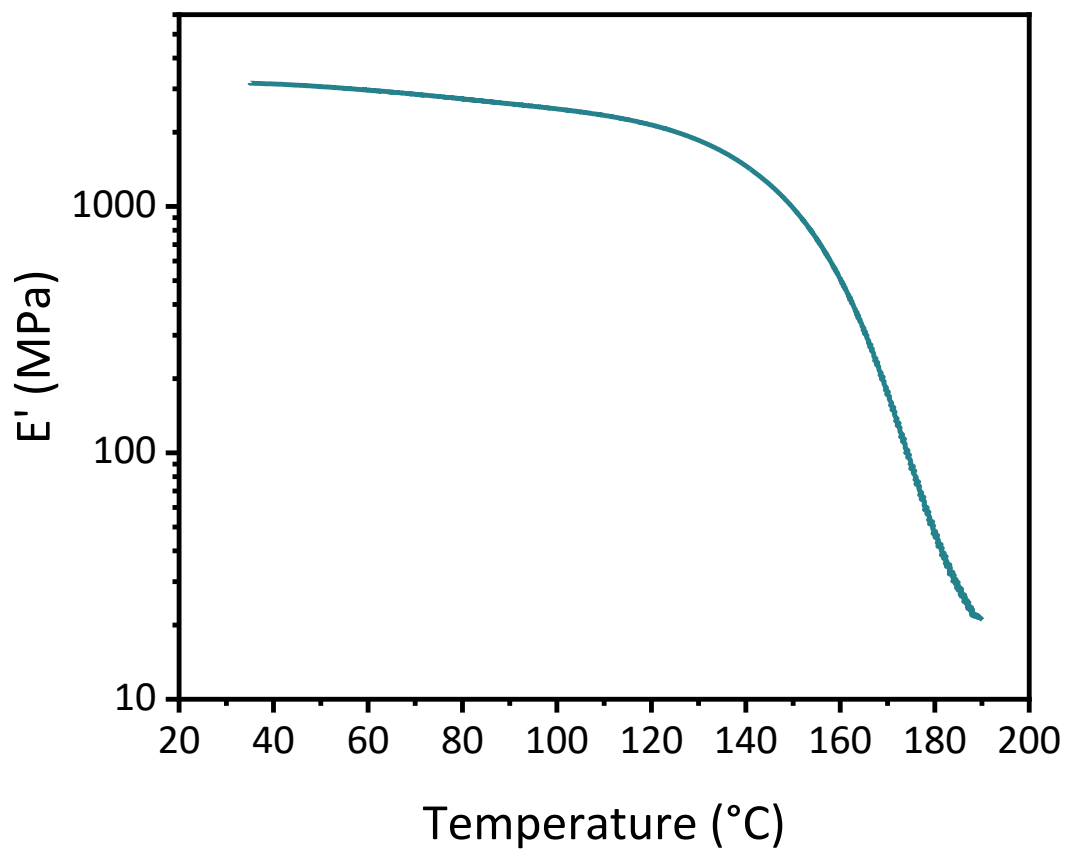


**Figure S17.** DMA thermogram of storage modulus versus temperature for representative sample of CAN A<sub>0</sub>.

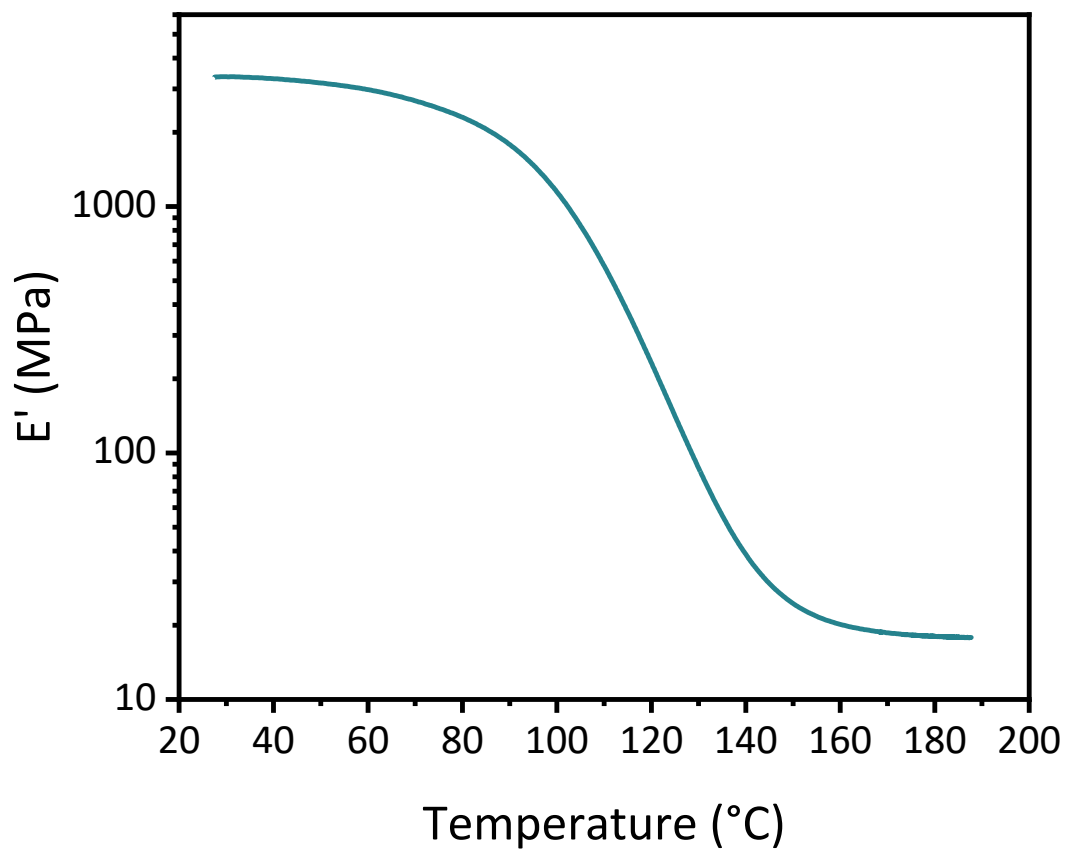


**Figure S18.** DMA thermogram of storage modulus versus temperature for representative sample of CAN A<sub>5</sub>.

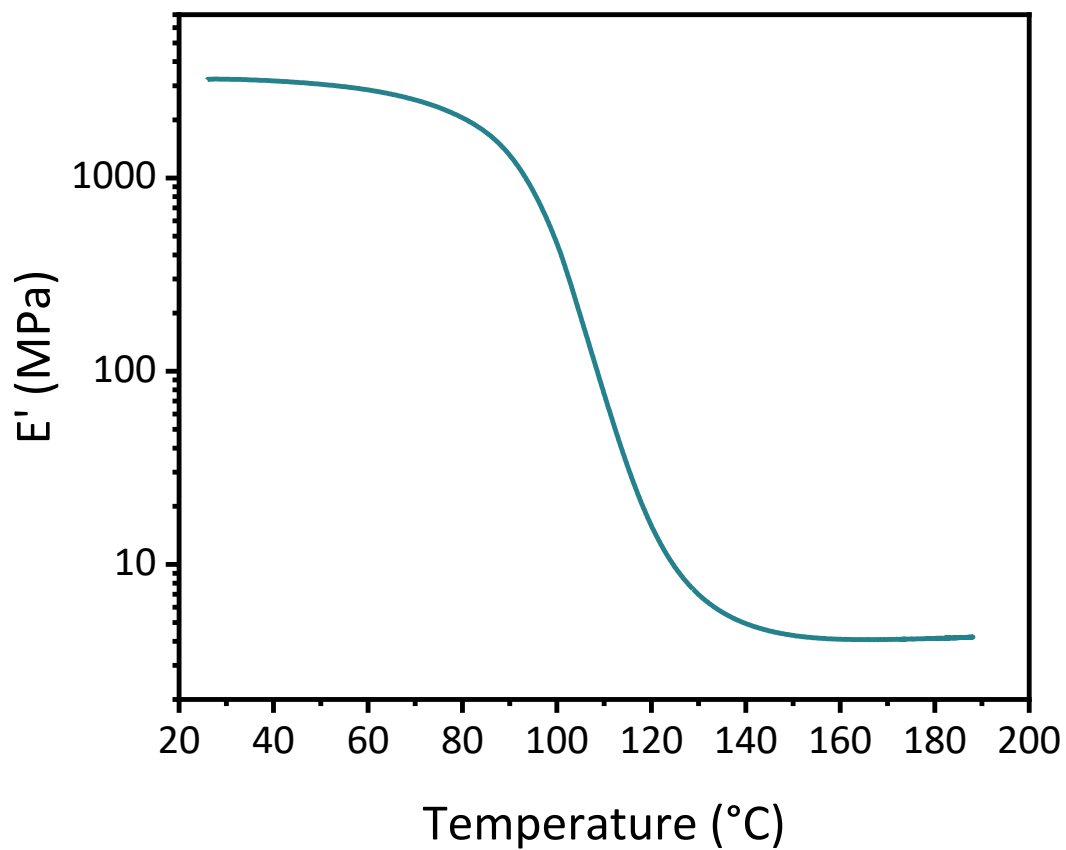


**Figure S19.** DMA thermogram of storage modulus versus temperature for representative sample of CAN B<sub>5</sub>.

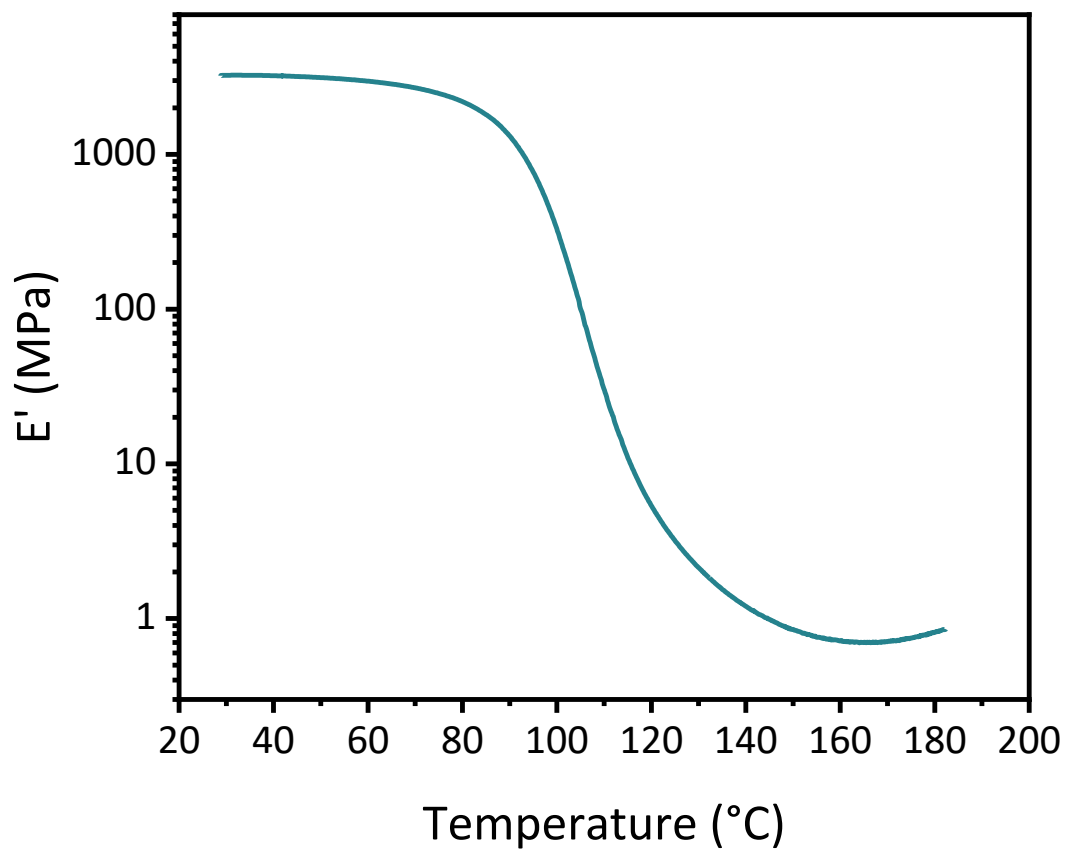


**Figure S20.** DMA thermogram of storage modulus versus temperature for representative sample of CAN C<sub>5</sub>.

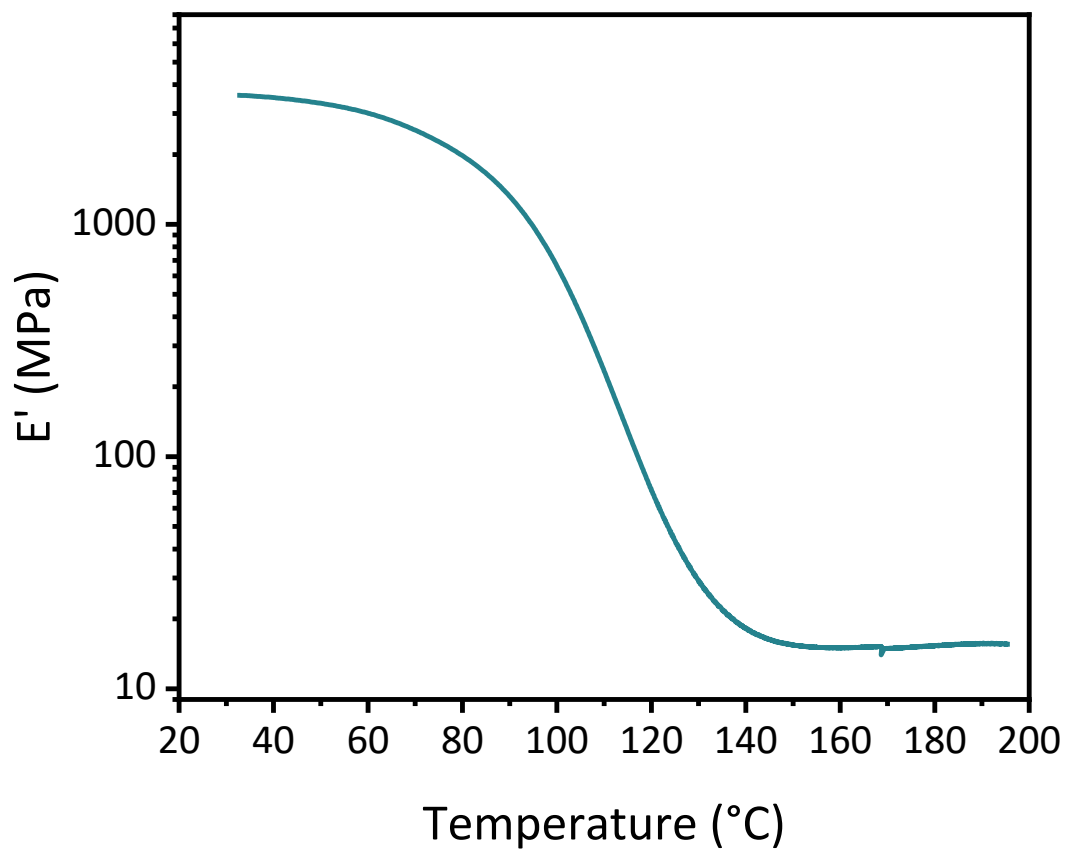


**Figure S21.** DMA thermogram of storage modulus versus temperature for representative sample of CAN A<sub>10</sub>.

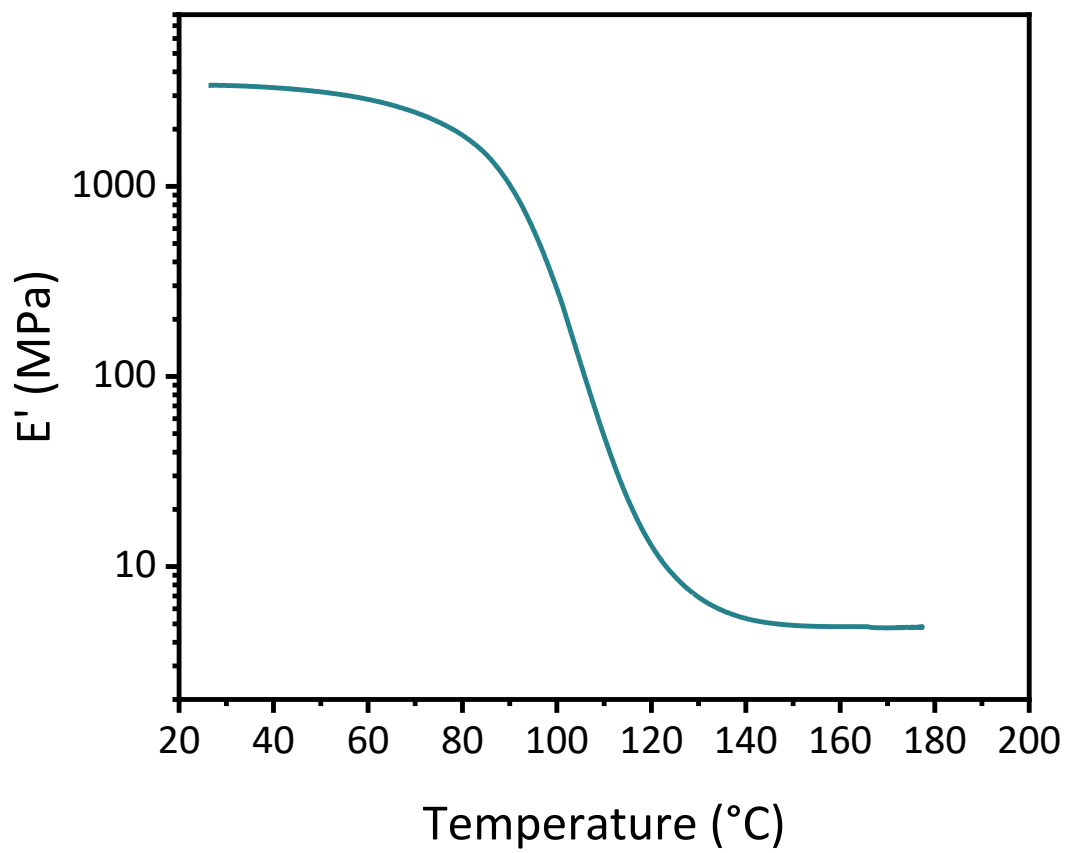


**Figure S22.** DMA thermogram of storage modulus versus temperature for representative sample of CAN B<sub>10</sub>.

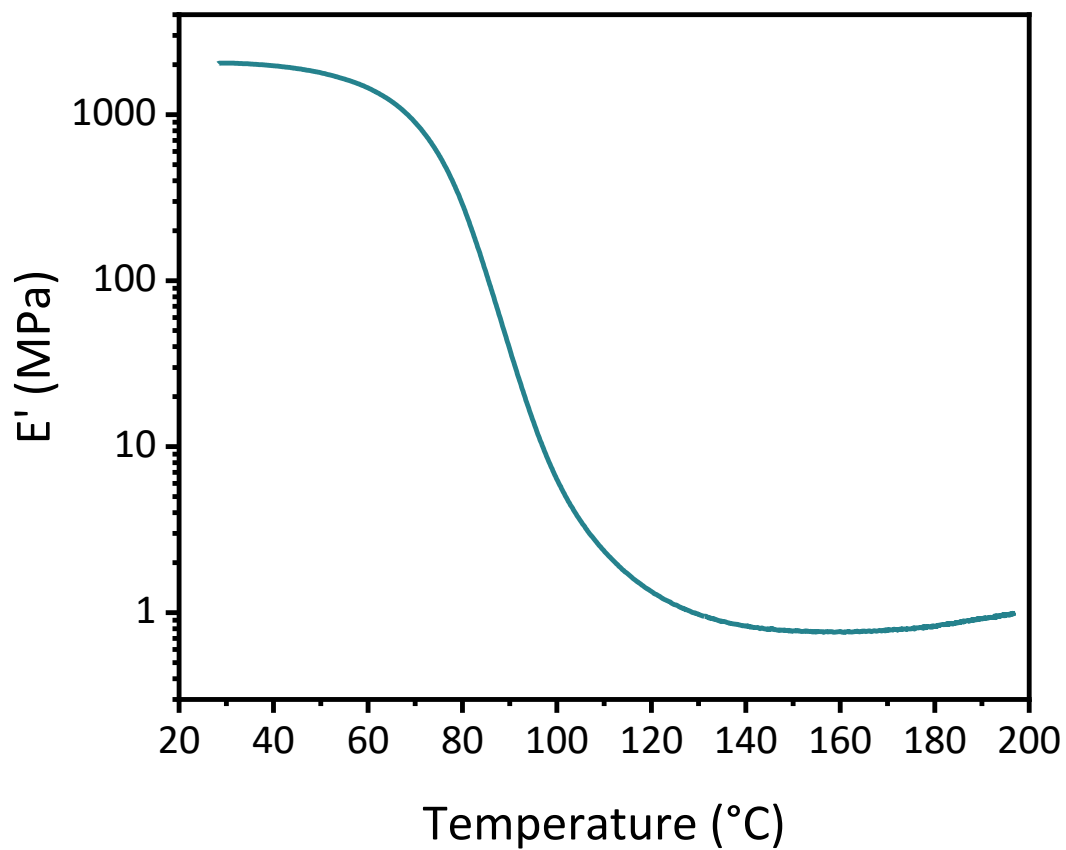


**Figure S23.** DMA thermogram of storage modulus versus temperature for representative sample of CAN C<sub>10</sub>.

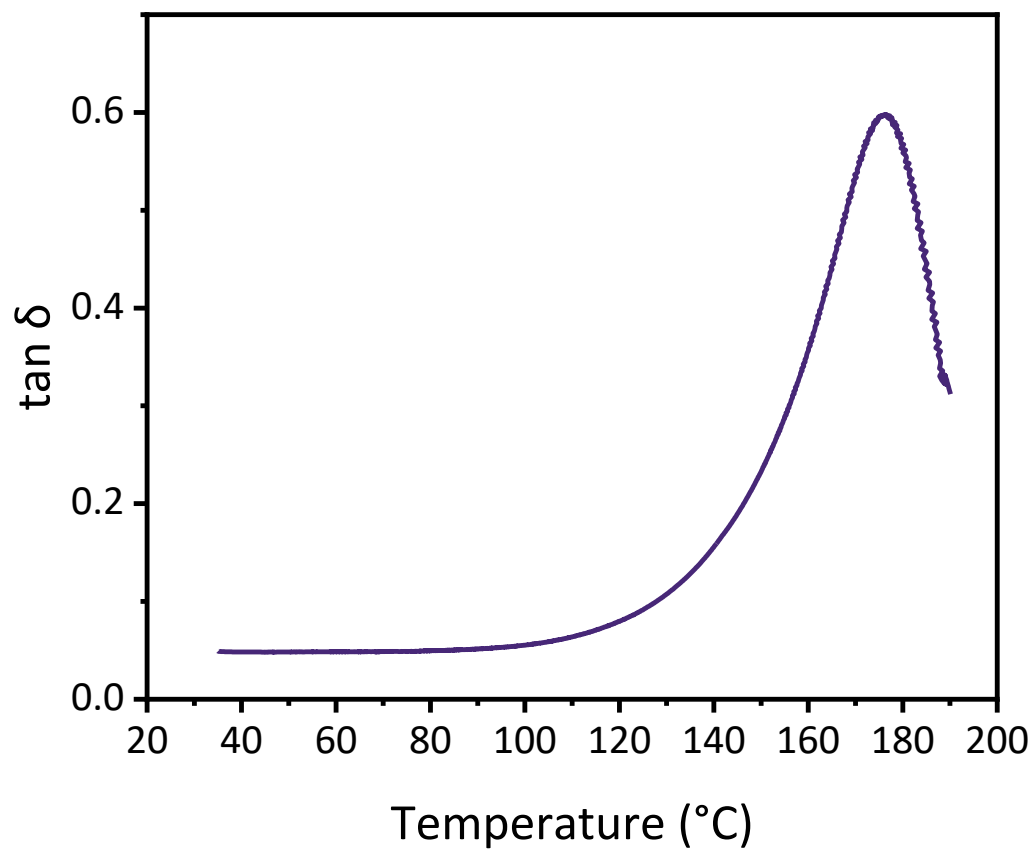


**Figure S24.** DMA thermogram of  $\tan \delta$  versus temperature for representative sample of CAN A<sub>0</sub>.  $T_g$  is taken as the peak of  $\tan \delta$ ;  $T_g = 176$  °C.



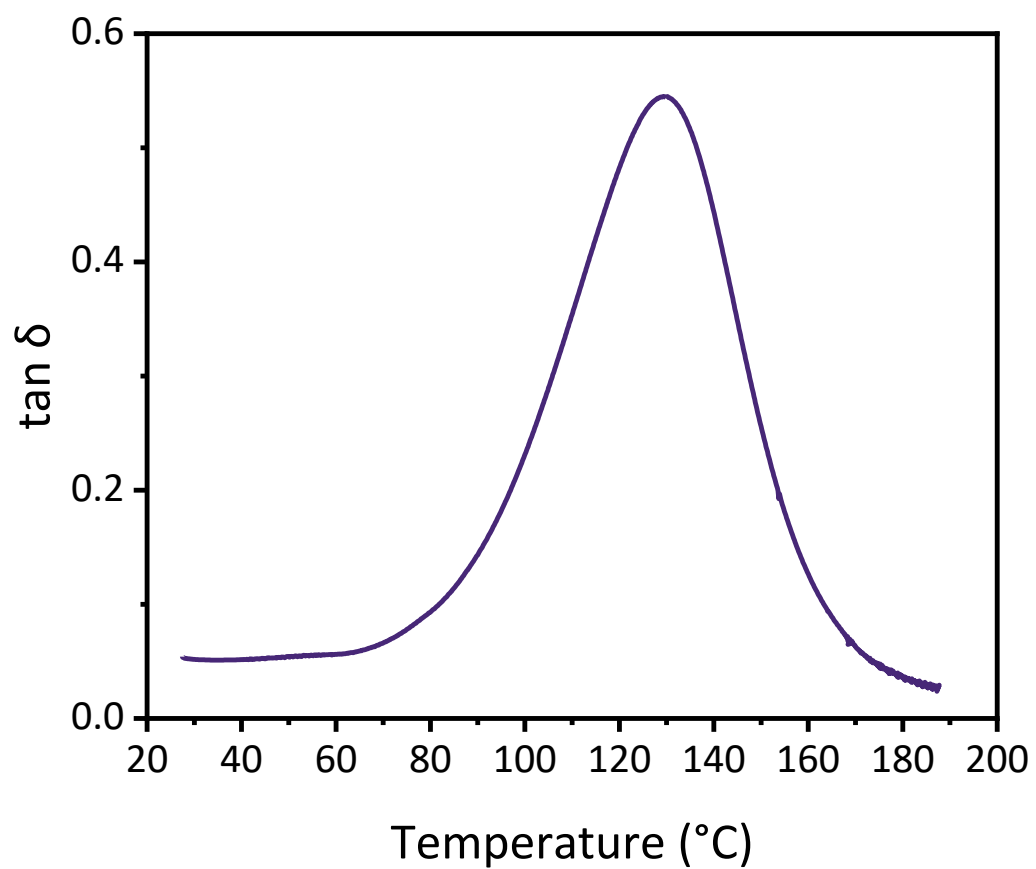


**Figure S25.** DMA thermogram of  $\tan \delta$  versus temperature for representative sample of CAN A<sub>5</sub>.  $T_g$  is taken as the peak of  $\tan \delta$ ;  $T_g = 130$  °C.

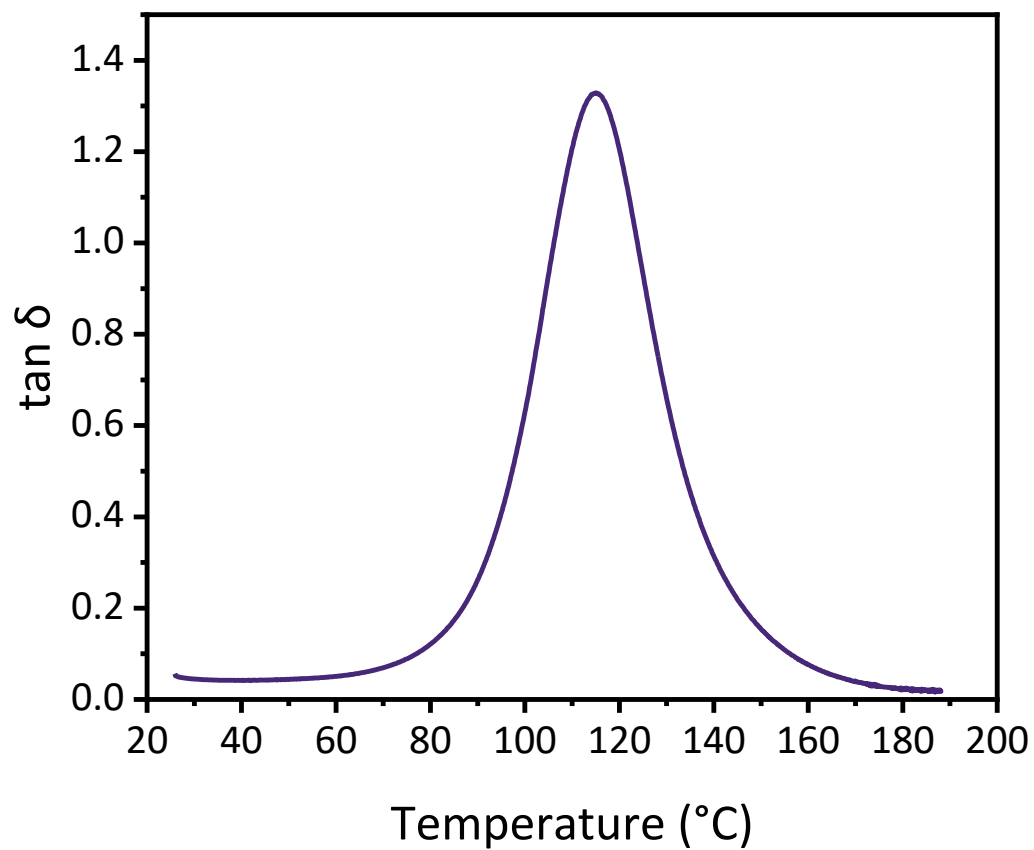


**Figure S26.** DMA thermogram of  $\tan \delta$  versus temperature for representative sample of CAN B<sub>5</sub>.  $T_g$  is taken as the peak of  $\tan \delta$ ;  $T_g = 116$  °C.

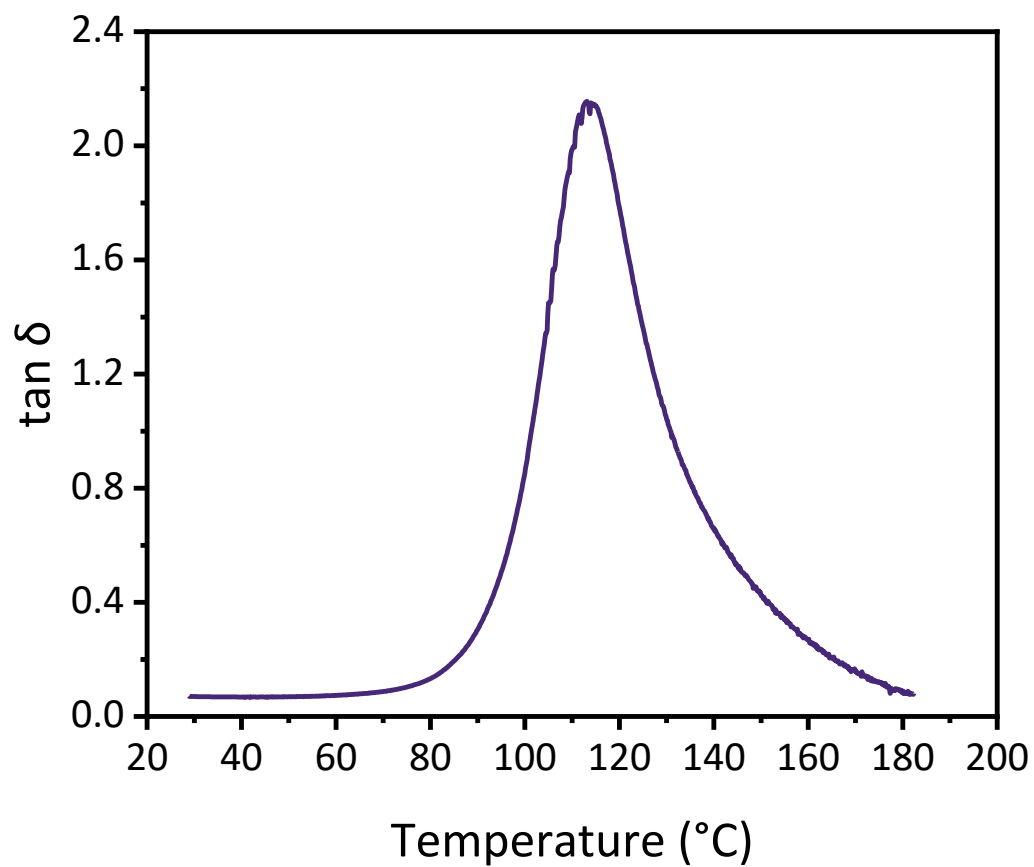


**Figure S27.** DMA thermogram of  $\tan \delta$  versus temperature for representative sample of CAN C<sub>5</sub>.  $T_g$  is taken as the peak of  $\tan \delta$ ;  $T_g = 114$  °C.

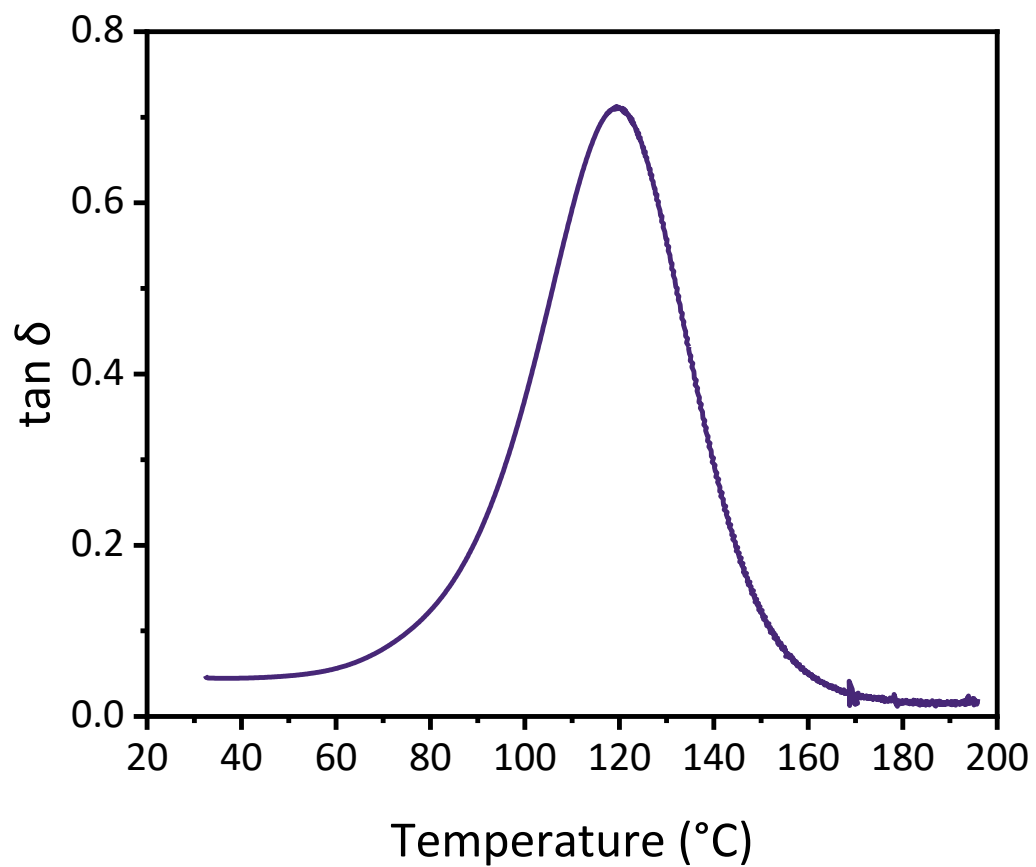


**Figure S28.** DMA thermogram of  $\tan \delta$  versus temperature for representative sample of CAN A<sub>10</sub>.  $T_g$  is taken as the peak of  $\tan \delta$ ;  $T_g = 120$  °C.

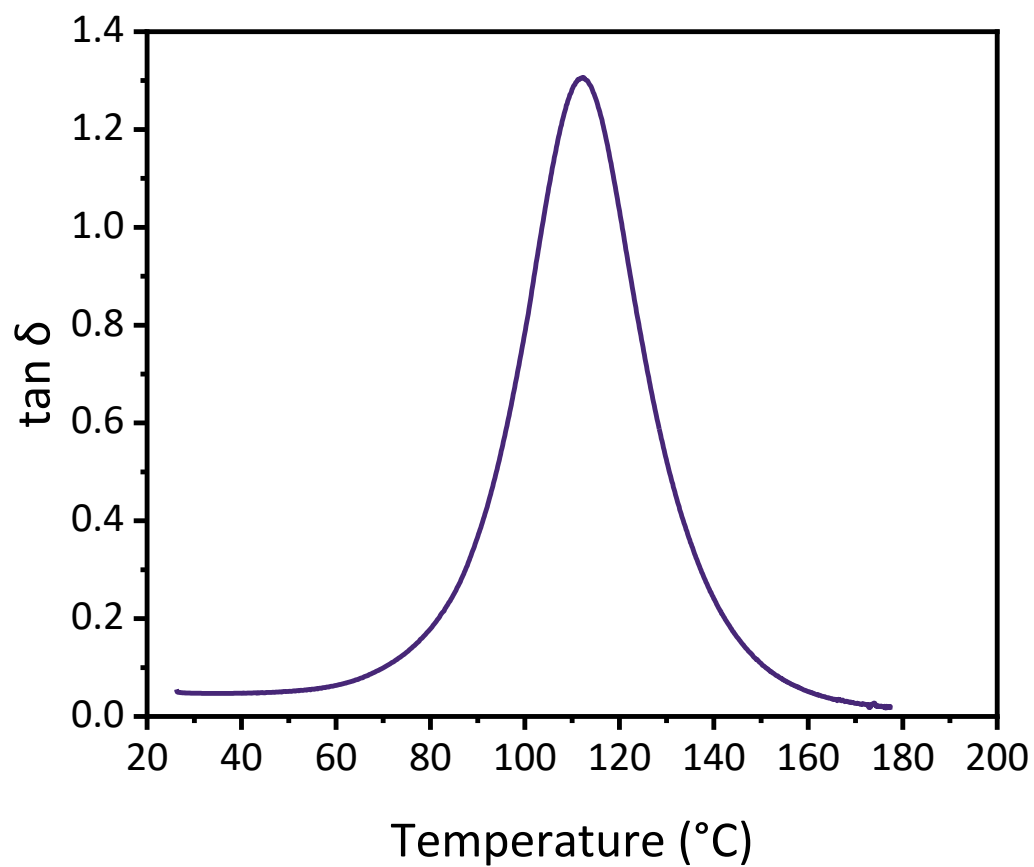


**Figure S29.** DMA thermogram of  $\tan \delta$  versus temperature for representative sample of CAN B<sub>10</sub>.  $T_g$  is taken as the peak of  $\tan \delta$ ;  $T_g = 112$  °C.

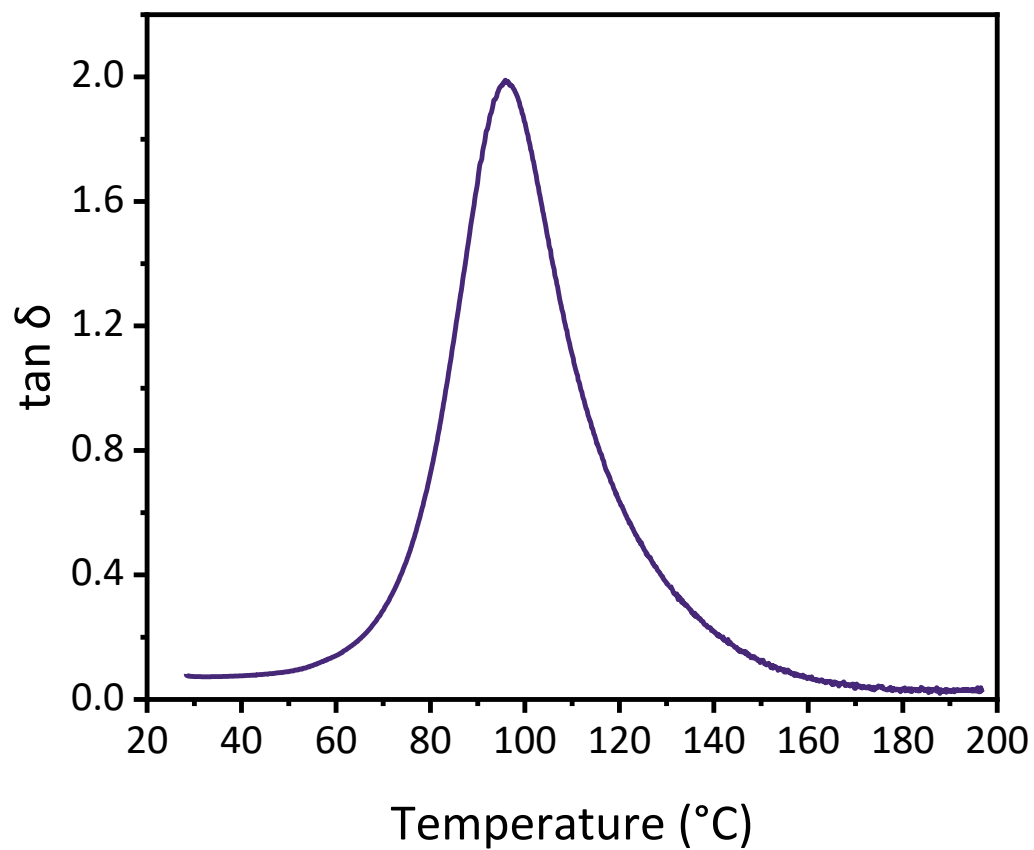


**Figure S30.** DMA thermogram of  $\tan \delta$  versus temperature for representative sample of CAN C<sub>10</sub>.  $T_g$  is taken as the peak of  $\tan \delta$ ;  $T_g = 96$  °C.

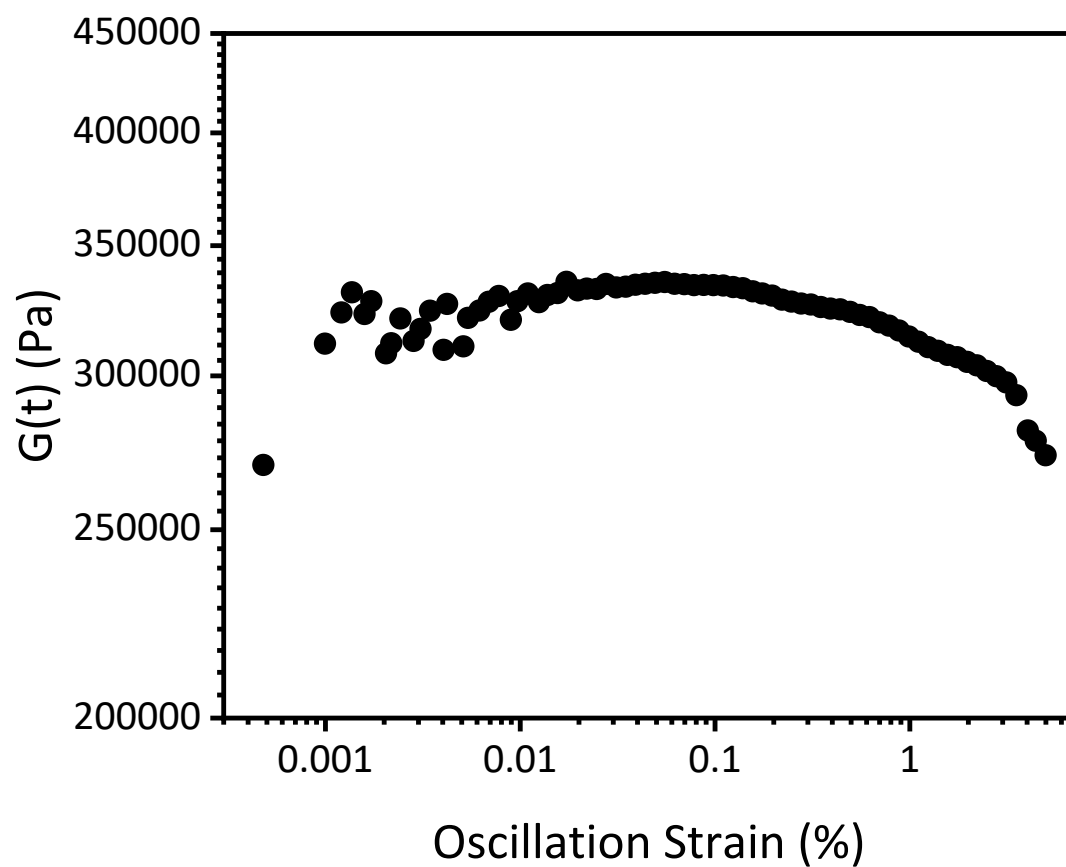


Figure S31. Strain sweep data for a representative sample of CAN A<sub>5</sub>.

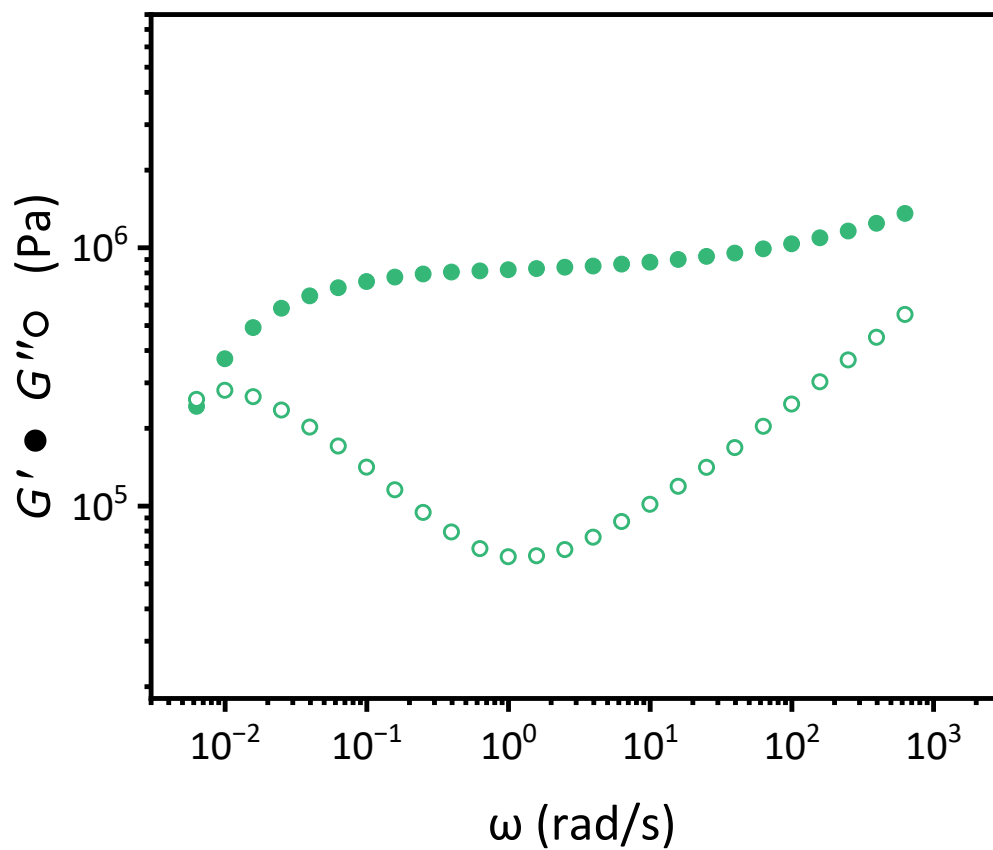


Figure S32. Frequency sweep performed at 175 °C for a representative sample of CAN A<sub>5</sub>.  $\tau^*_{cross} = 146$  s.



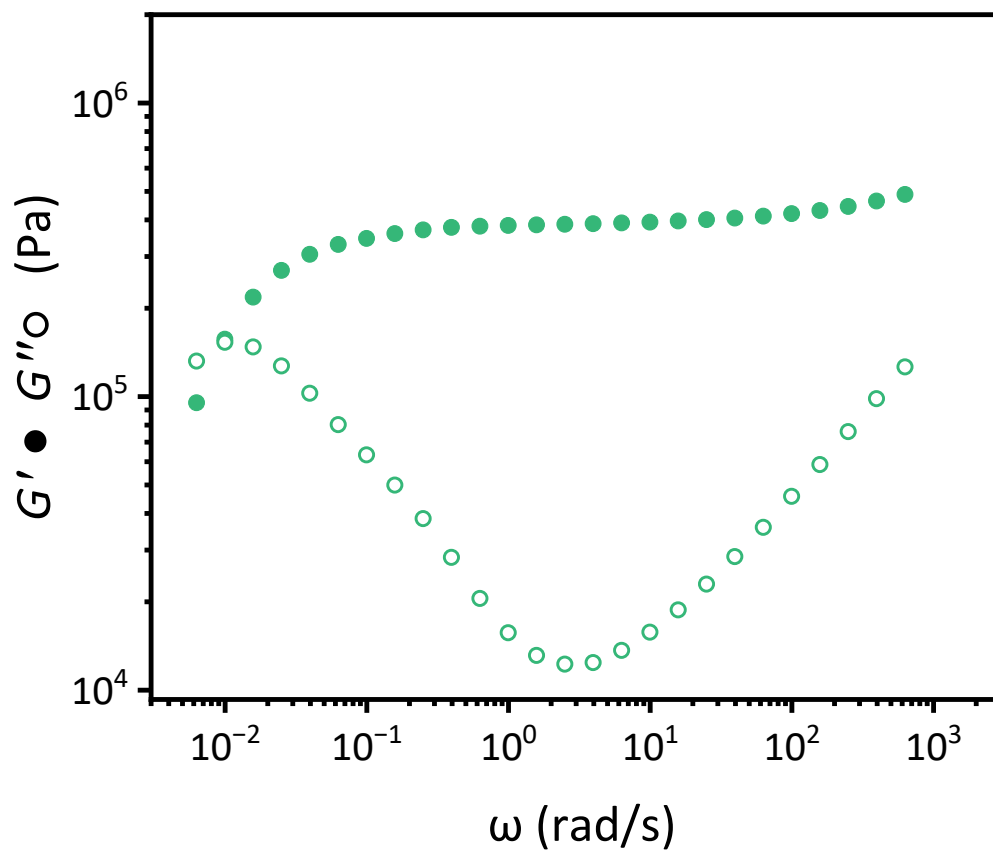


Figure S33. Frequency sweep performed at 175 °C for a representative sample of CAN B<sub>5</sub>.  $\tau^*_{\text{cross}} = 104$  s.

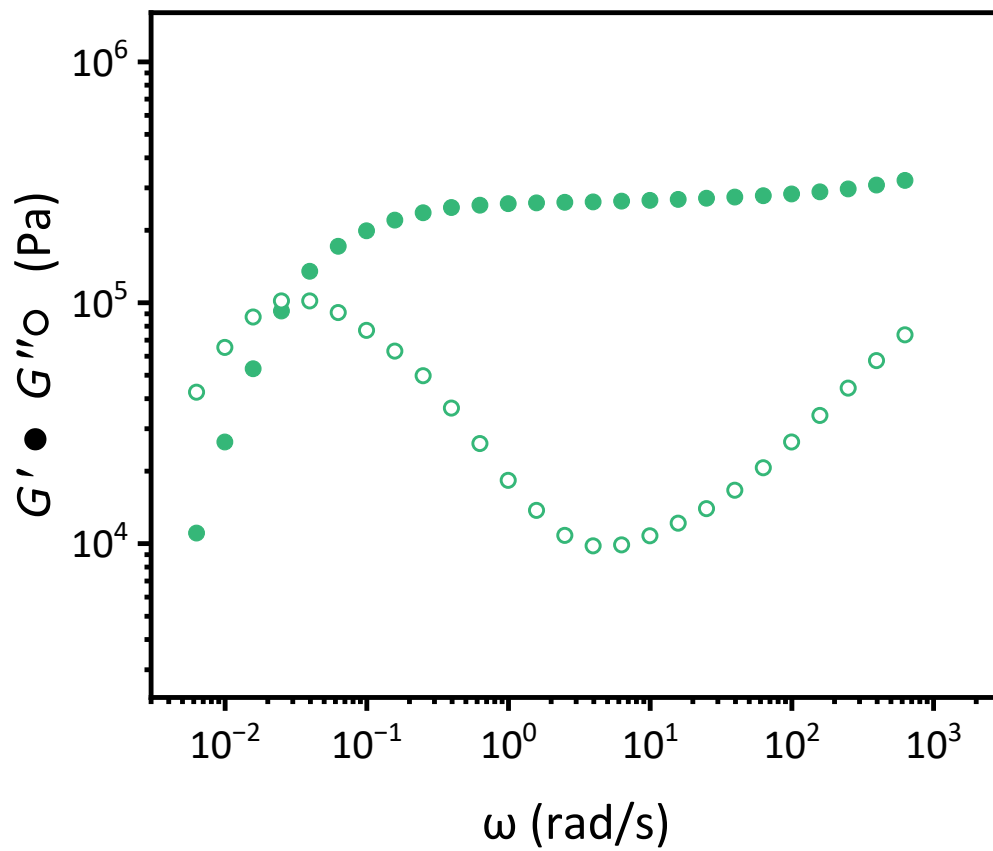


Figure S34. Frequency sweep performed at 175 °C for a representative sample of CAN C<sub>5</sub>.  $\tau^*_{\text{cross}} = 36$  s.

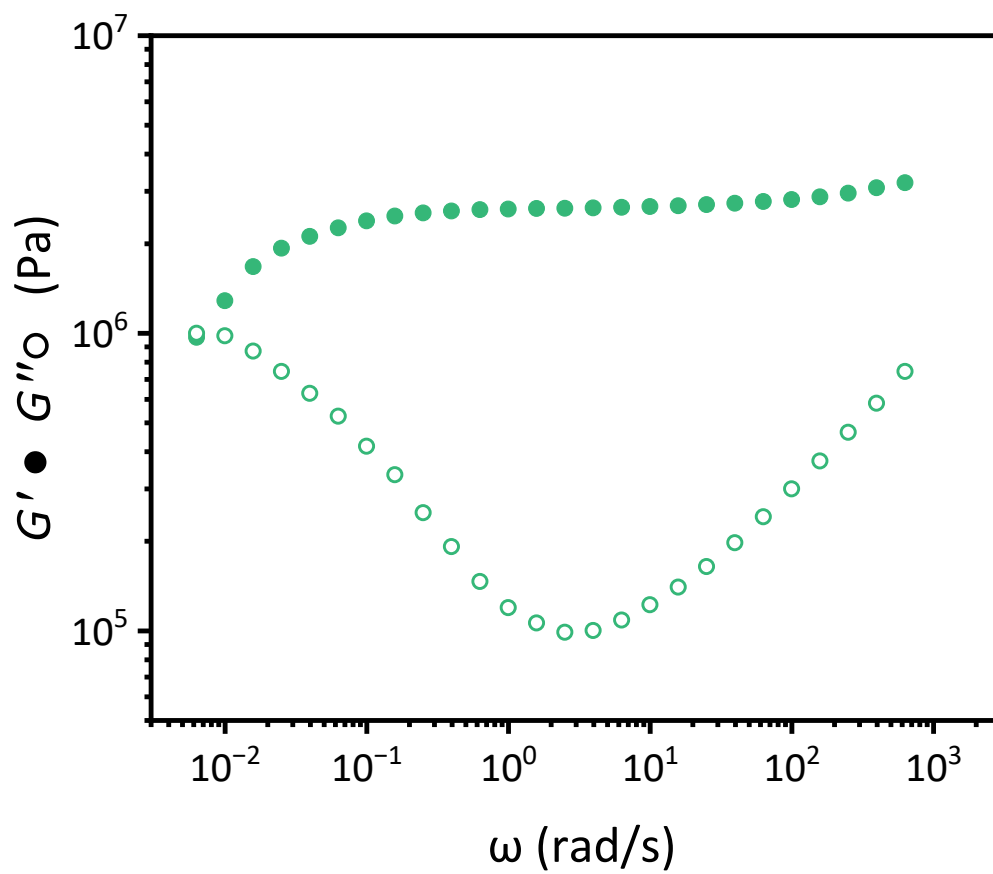


Figure S35. Frequency sweep performed at 175 °C for a representative sample of CAN A<sub>10</sub>.  $\tau^*_{\text{cross}} = 152$  s.

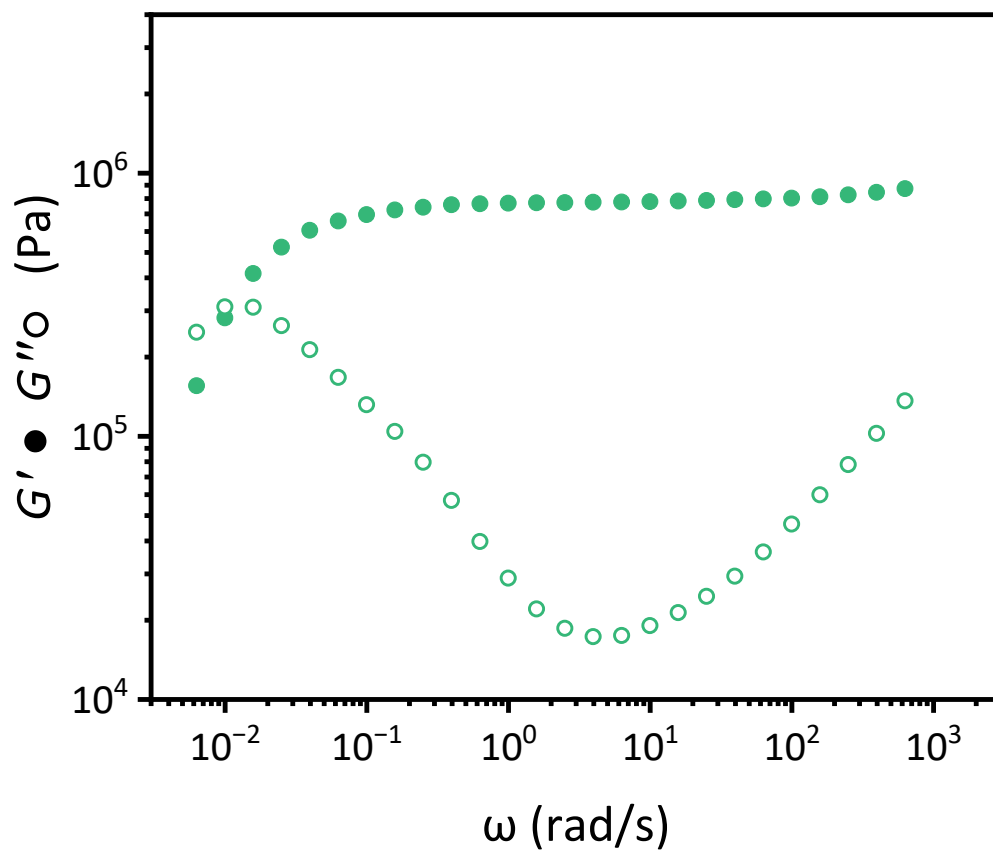


Figure S36. Frequency sweep performed at 175 °C for a representative sample of CAN B<sub>10</sub>.  $\tau^*_{\text{cross}} = 90$  s.

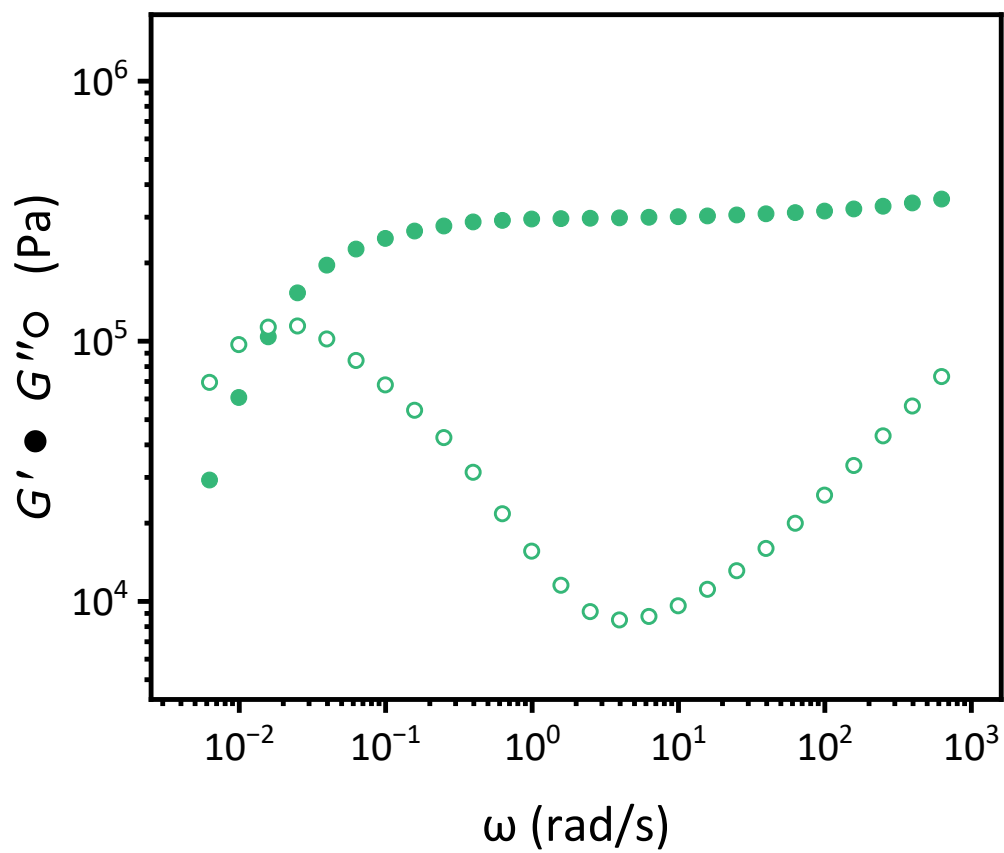
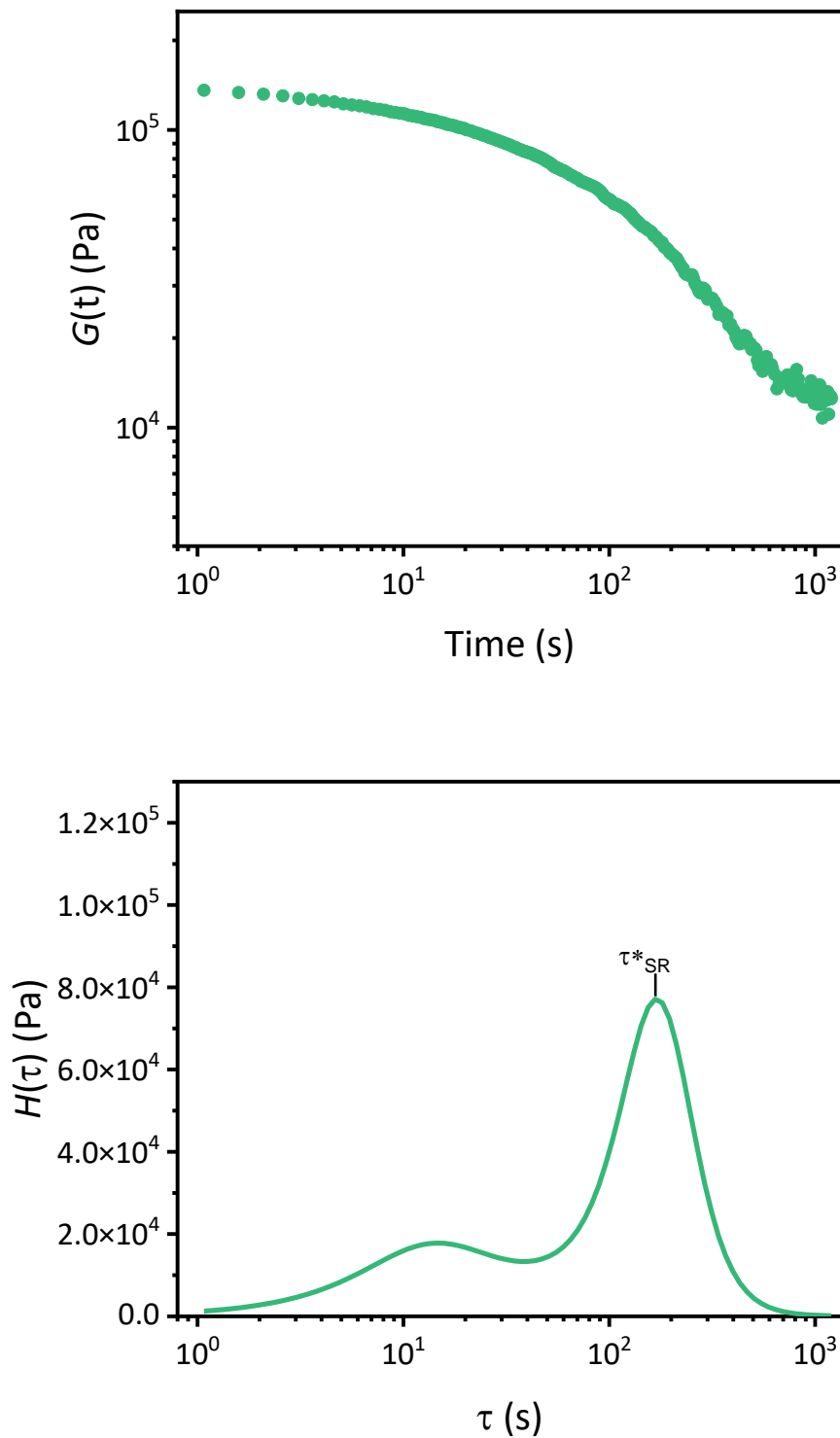
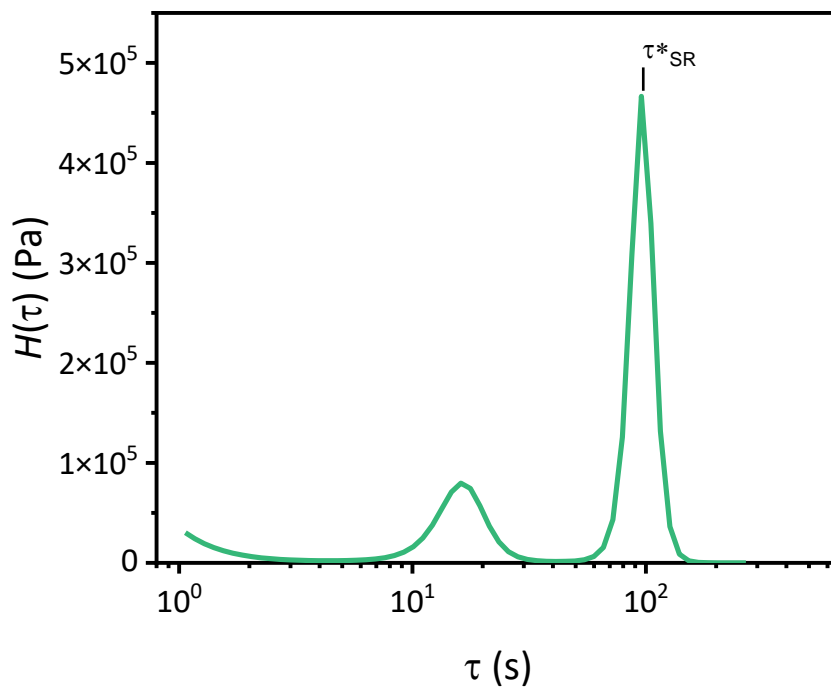
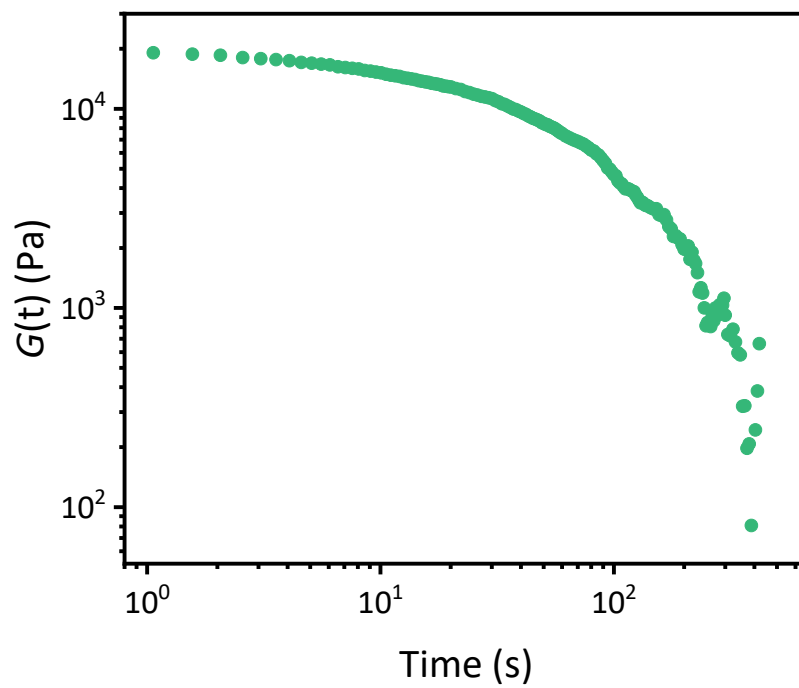


Figure S37. Frequency sweep performed at 175 °C for a representative sample of CAN C<sub>10</sub>.  $\tau^*_{\text{cross}} = 57$  s.



**Figure S38.** Stress relaxation and calculated continuous relaxation spectrum at 175 °C for a representative sample of CAN A<sub>5</sub>.  $\tau^*_{SR} = 167$  s.



**Figure S39.** Stress relaxation and calculated continuous relaxation spectrum at 175 °C for a representative sample of CAN B<sub>5</sub>.  $\tau^*_{SR} = 96$  s.

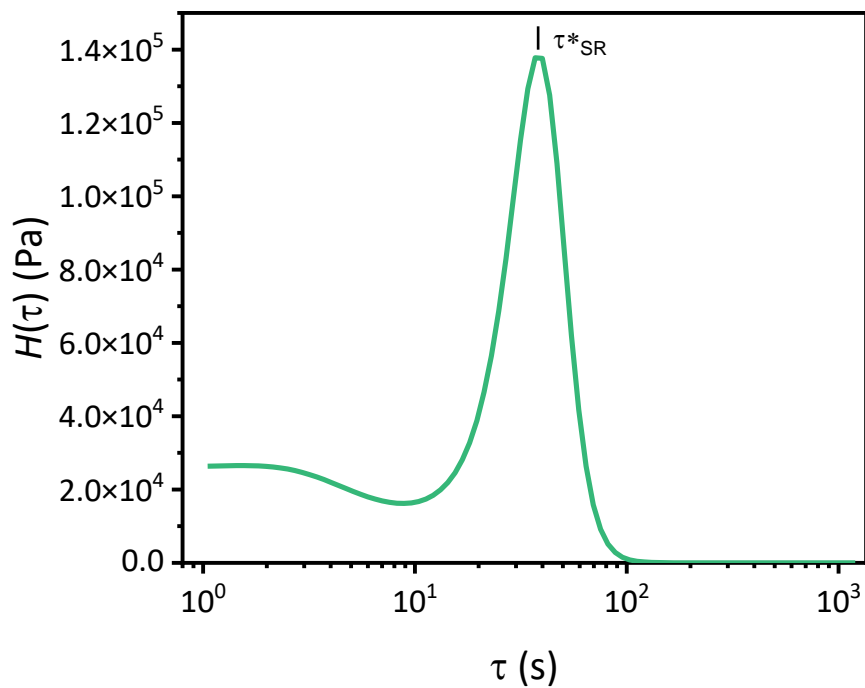
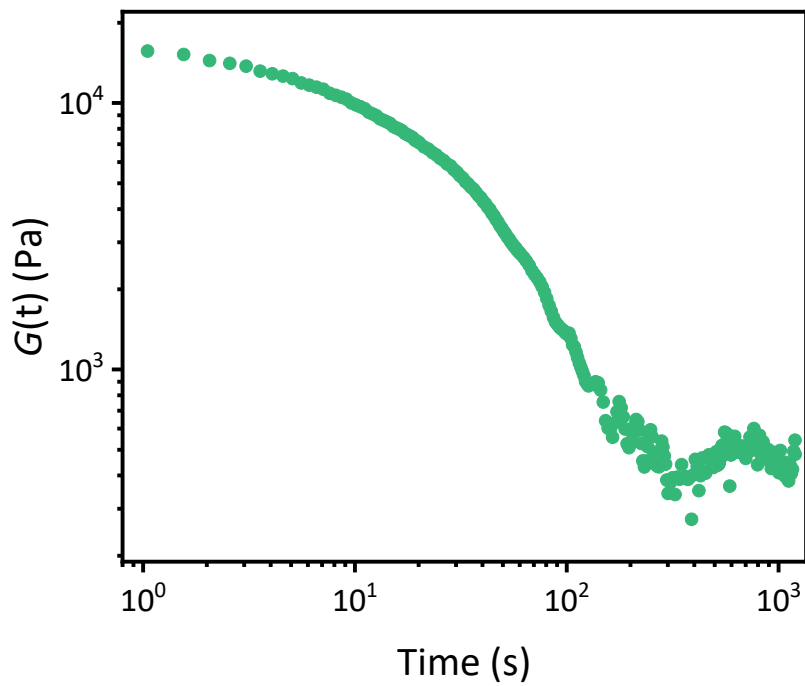


**Figure S40.** Stress relaxation and calculated continuous relaxation spectrum at 175 °C for a representative sample of CAN C<sub>5</sub>.  $\tau^*_{SR} = 40$  s.



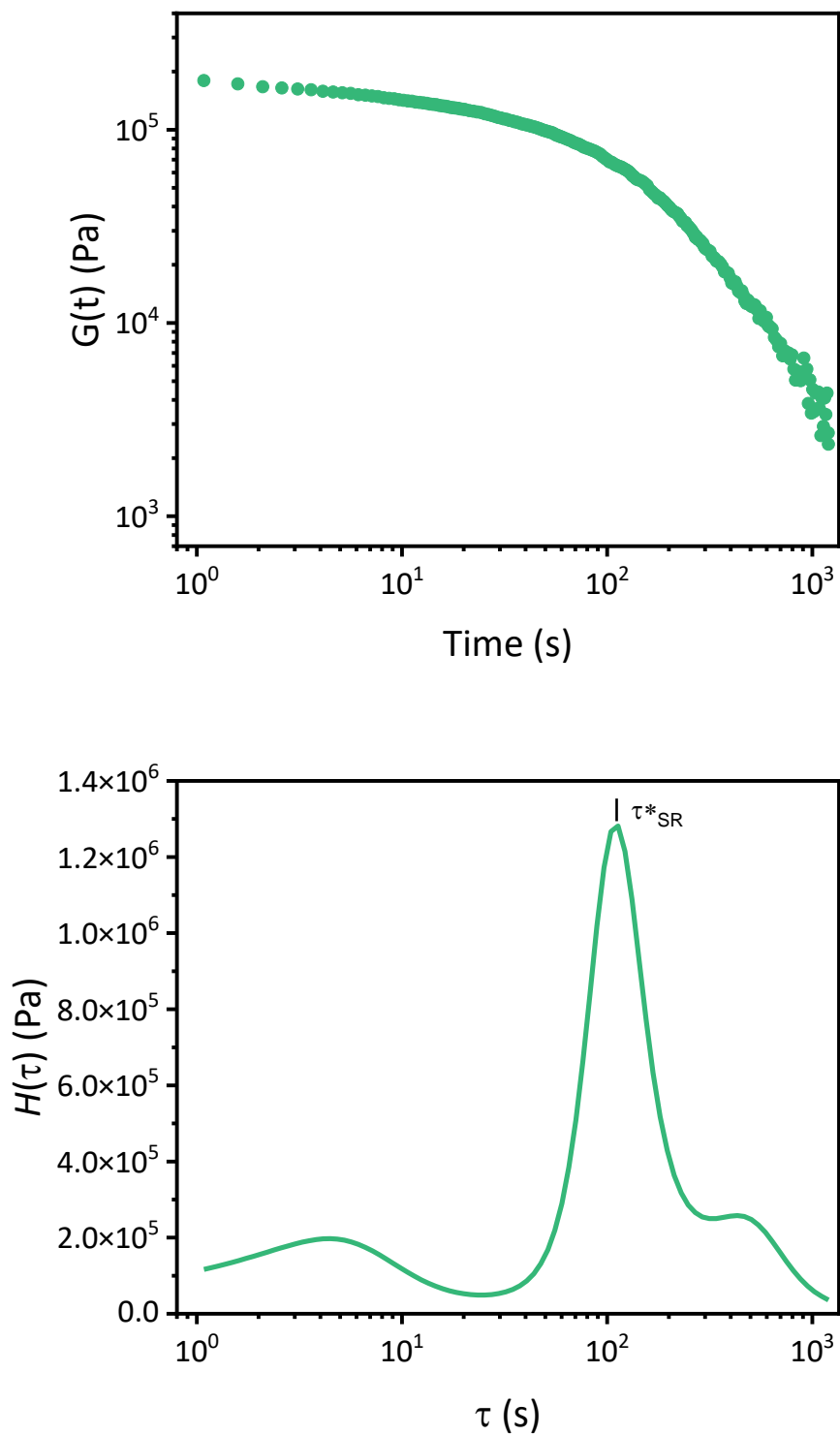


**Figure S41.** Stress relaxation and calculated continuous relaxation spectrum at 175 °C for a representative sample of CAN A<sub>10</sub>.  $\tau^*_{SR} = 113$  s.

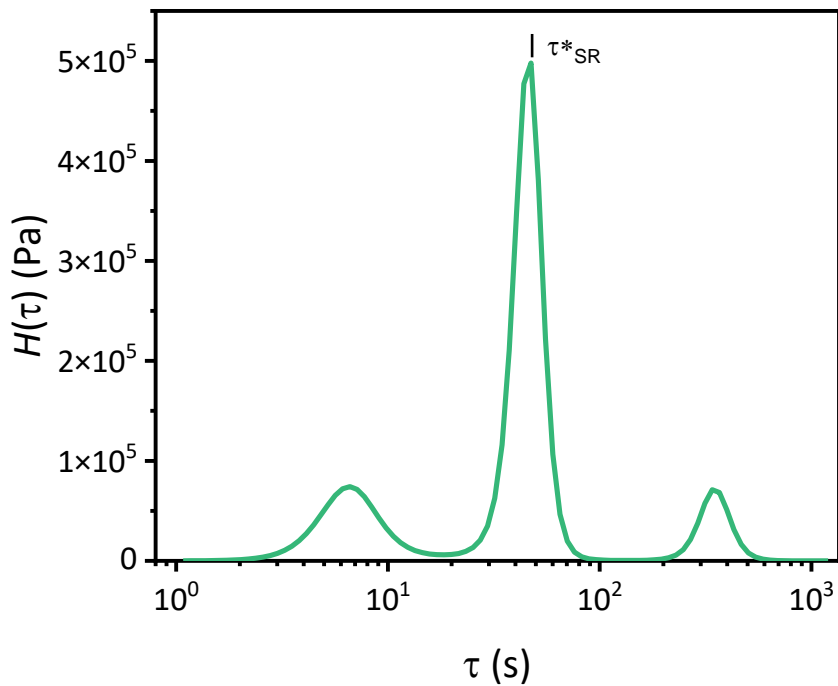
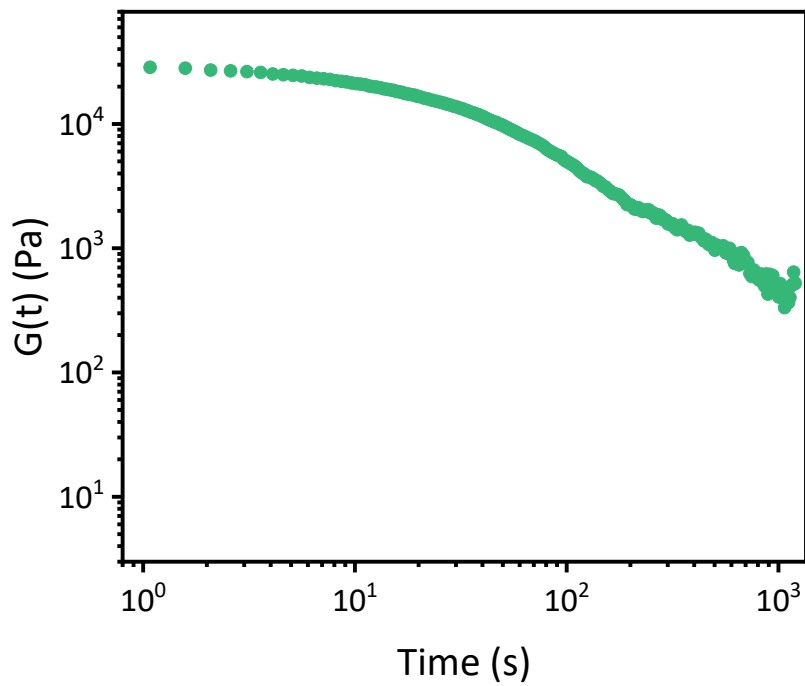


**Figure S42.** Stress relaxation and calculated continuous relaxation spectrum at 175 °C for a representative sample of CAN B<sub>10</sub>.  $\tau^*_{SR} = 48$  s.

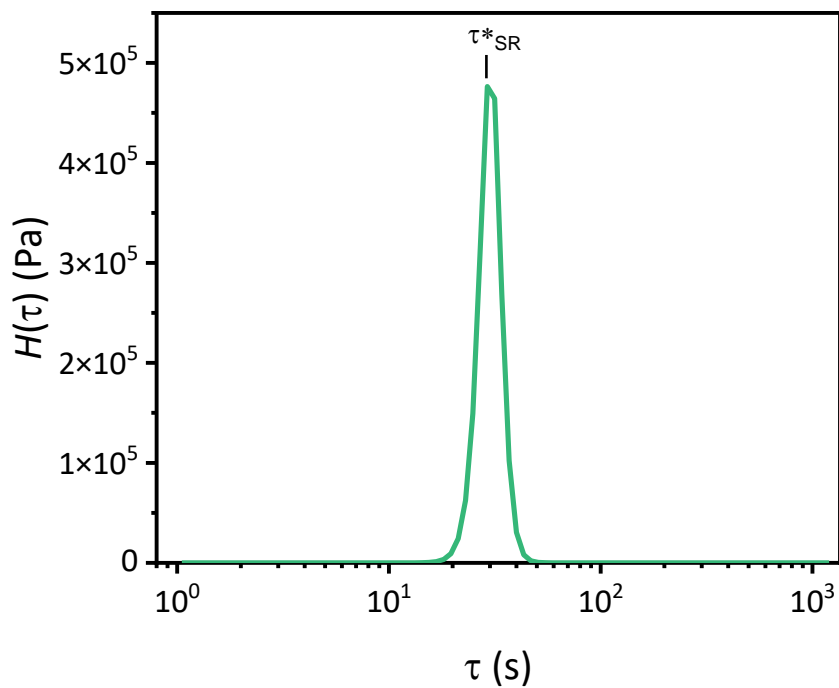
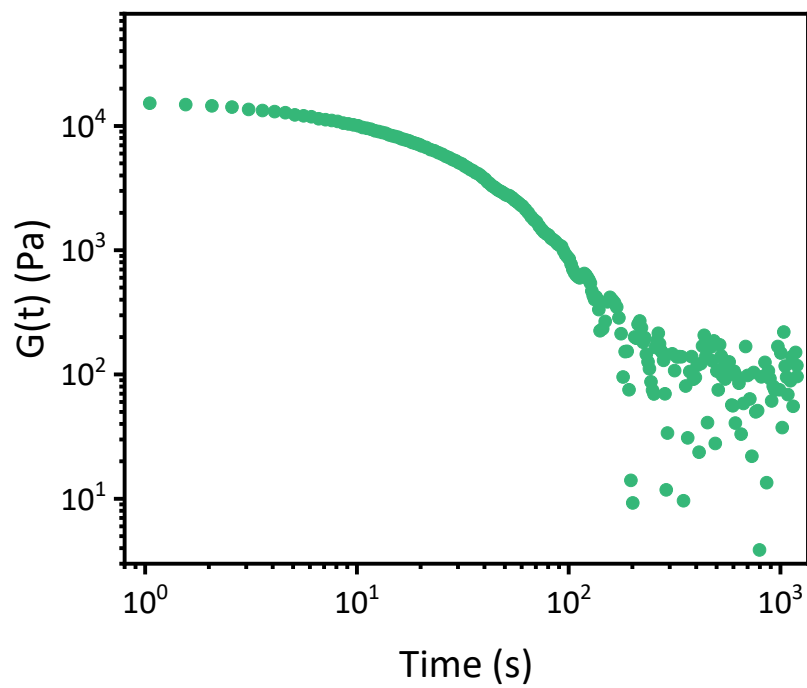


**Figure S43.** Stress relaxation and calculated continuous relaxation spectrum at 175 °C for a representative sample of CAN C<sub>10</sub>.  $\tau^*_{SR} = 29$  s.

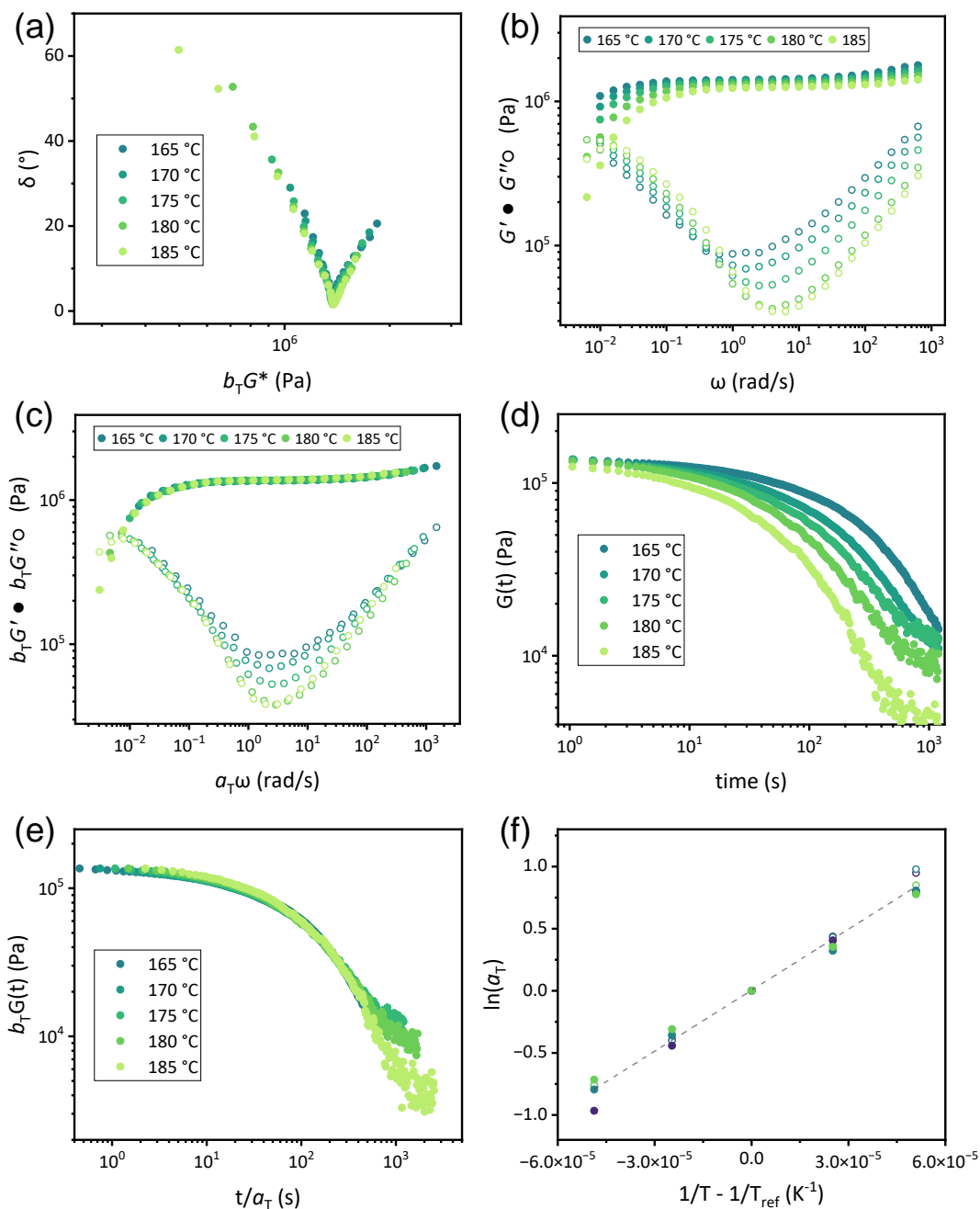


**Figure S44.** (a) Reduced van Gurp-Palmen plot of a sample of CAN A<sub>5</sub>. (b) Unshifted frequency sweep data of a sample of CAN A<sub>5</sub>. (c) Master curve of frequency sweep data constructed via TTS of a sample of CAN A<sub>5</sub>. (d) Unshifted stress relaxation data of a sample of CAN A<sub>5</sub>. (e) Master curve of stress relaxation constructed from TTS of a sample of CAN A<sub>5</sub>. (f) Arrhenius analysis of horizontal shift factors for all CAN A<sub>5</sub> samples. Filled circles are from frequency sweep data and empty circles from stress relaxation; each color is a single sample. Dashed line is line of best fit.  $T_{ref} = 175$  °C for all analyses.

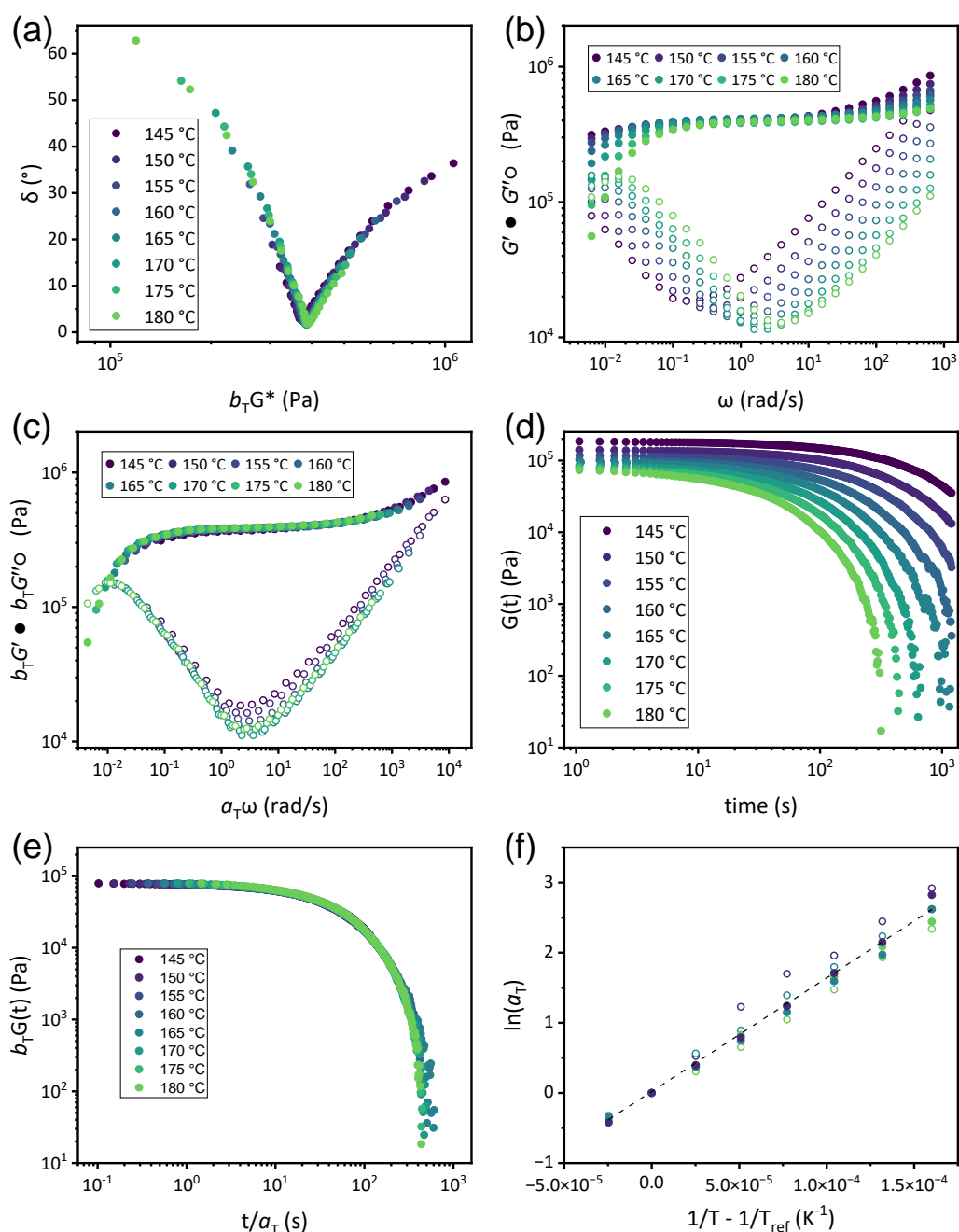


**Figure S45.** (a) Reduced van Gurp-Palmen plot of a sample of CAN B<sub>5</sub>. (b) Unshifted frequency sweep data of a sample of CAN B<sub>5</sub>. (c) Master curve of frequency sweep data constructed via TTS of a sample of CAN B<sub>5</sub>. (d) Unshifted stress relaxation data of a sample of CAN B<sub>5</sub>. (e) Master curve of stress relaxation constructed from TTS of a sample of CAN B<sub>5</sub>. (f) Arrhenius analysis of horizontal shift factors for all CAN B<sub>5</sub> samples. Filled circles are from frequency sweep data and empty circles from stress relaxation; each color is a single sample. Dashed line is line of best fit.  $T_{ref} = 175$  °C for all analyses.

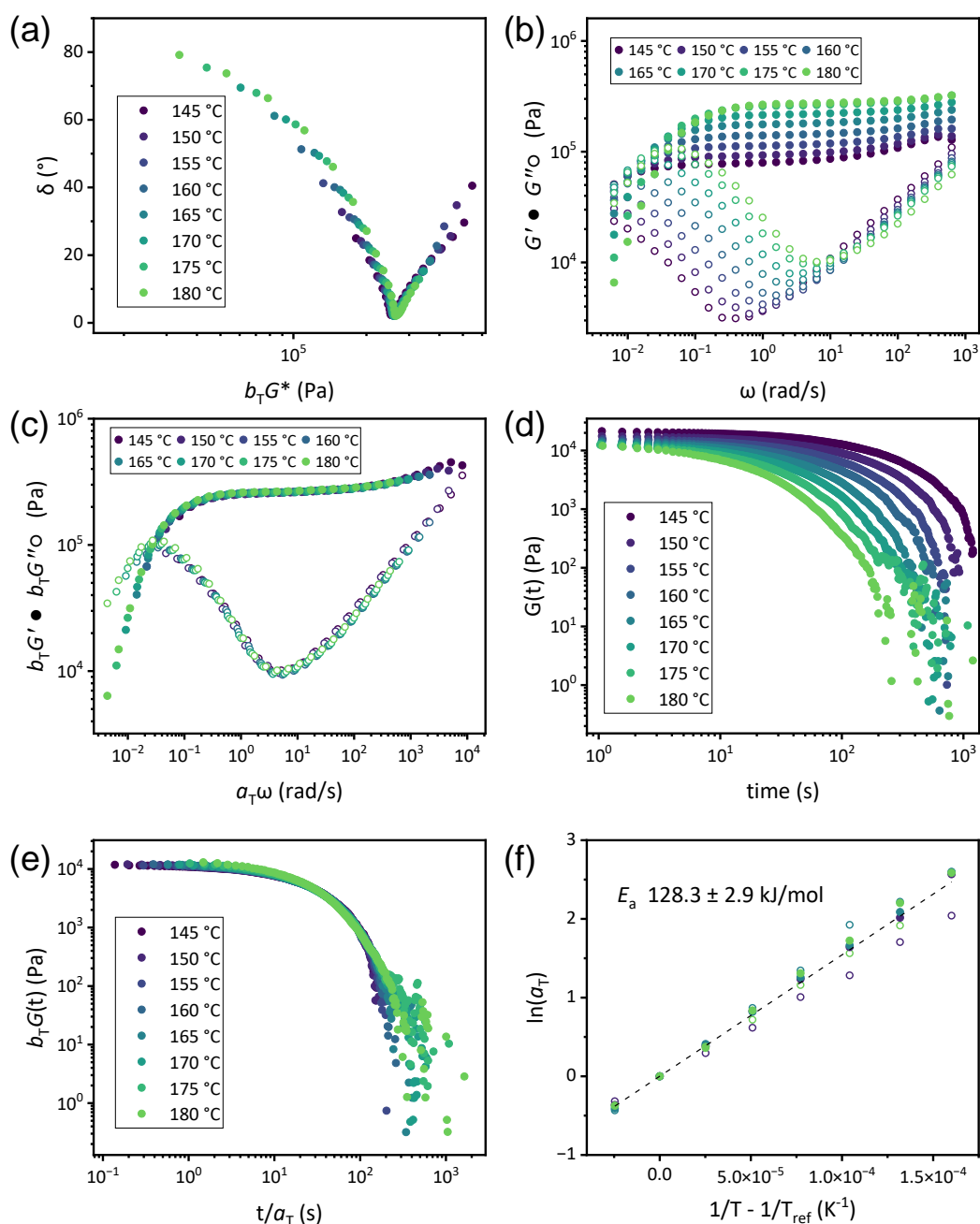


**Figure S46.** (a) Reduced van Gurp-Palmen plot of a sample of CAN C<sub>5</sub>. (b) Unshifted frequency sweep data of a sample of CAN C<sub>5</sub>. (c) Master curve of frequency sweep data constructed via TTS of a sample of CAN C<sub>5</sub>. (d) Unshifted stress relaxation data of a sample of CAN C<sub>5</sub>. (e) Master curve of stress relaxation constructed from TTS of a sample of CAN C<sub>5</sub>. (f) Arrhenius analysis of horizontal shift factors for all CAN C<sub>5</sub> samples. Filled circles are from frequency sweep data and empty circles from stress relaxation; each color is a single sample. Dashed line is line of best fit.  $T_{ref} = 175$  °C for all analyses. Figures a, c, e, and f are identical to main text Figure 4.

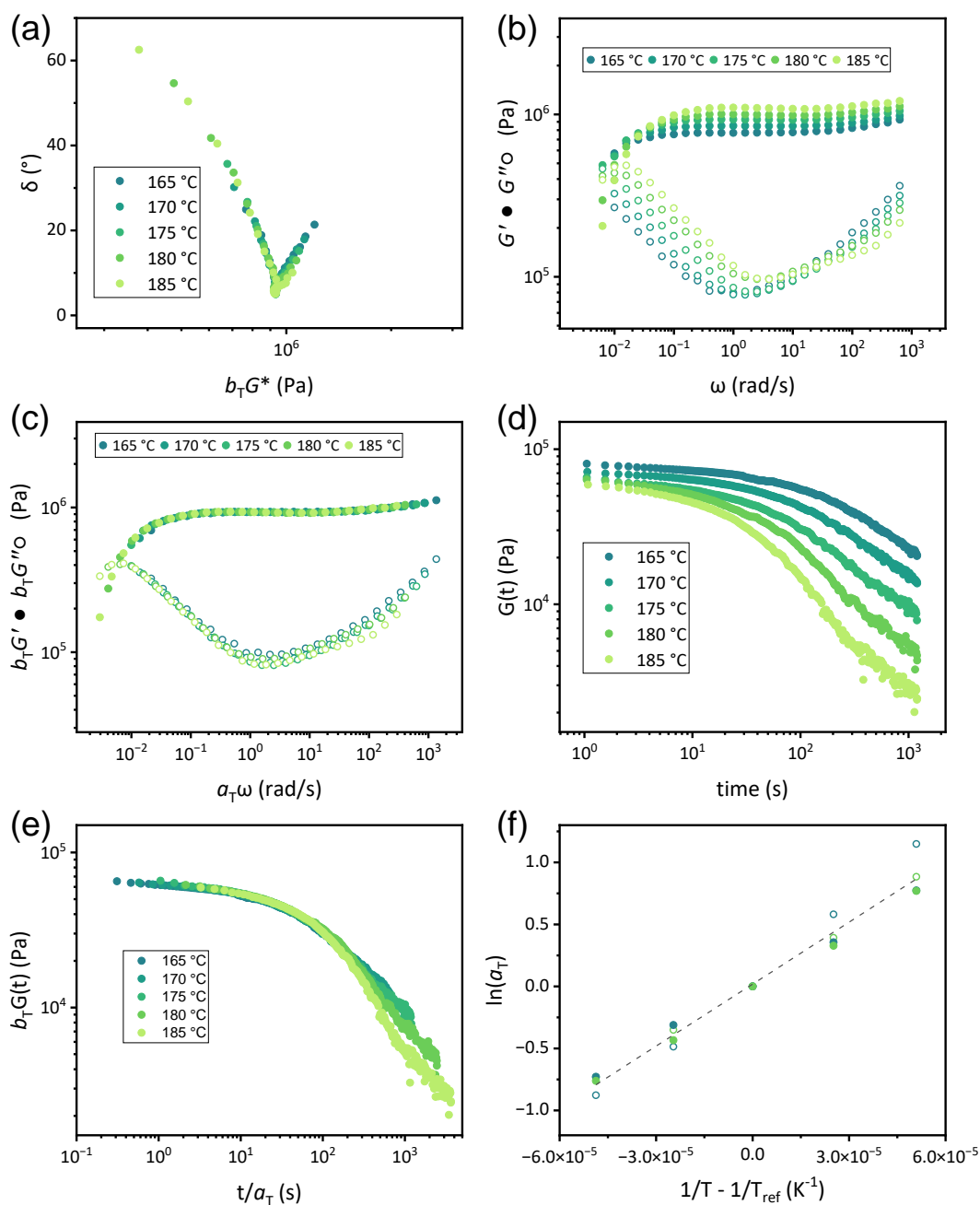


**Figure S47.** (a) Reduced van Gurp-Palmen plot of a sample of CAN A<sub>10</sub>. (b) Unshifted frequency sweep data of a sample of CAN A<sub>10</sub>. (c) Master curve of frequency sweep data constructed via TTS of a sample of CAN A<sub>10</sub>. (d) Unshifted stress relaxation data of a sample of CAN A<sub>10</sub>. (e) Master curve of stress relaxation constructed from TTS of a sample of CAN A<sub>10</sub>. (f) Arrhenius analysis of horizontal shift factors for all CAN A<sub>10</sub> samples. Filled circles are from frequency sweep data and empty circles from stress relaxation; each color is a single sample. Dashed line is line of best fit.  $T_{ref} = 175$  °C for all analyses.

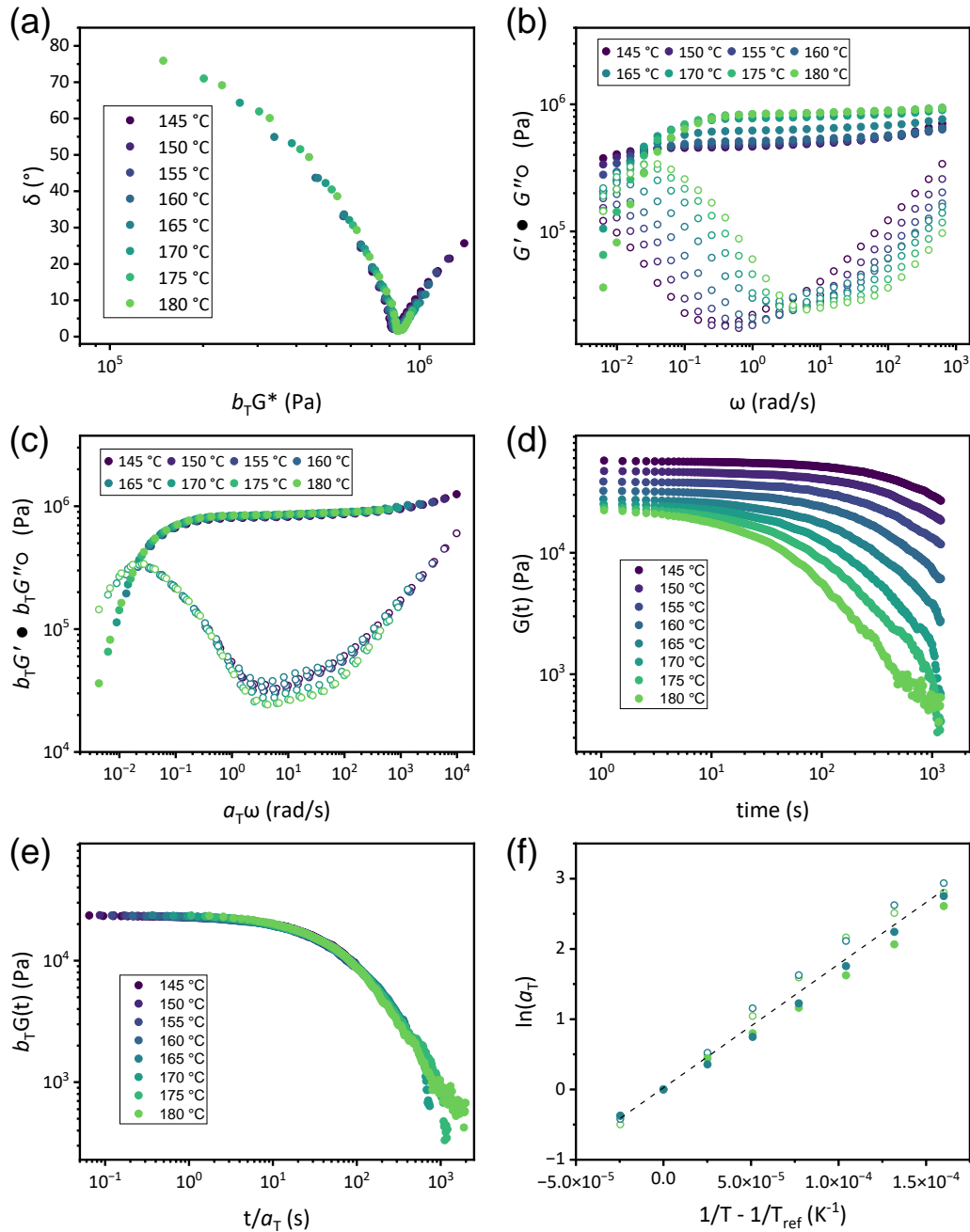


**Figure S48.** (a) Reduced van Gorp-Palmen plot of a sample of CAN B<sub>10</sub>. (b) Unshifted frequency sweep data of a sample of CAN B<sub>10</sub>. (c) Master curve of frequency sweep data constructed via TTS of a sample of CAN B<sub>10</sub>. (d) Unshifted stress relaxation data of a sample of CAN B<sub>10</sub>. (e) Master curve of stress relaxation constructed from TTS of a sample of CAN B<sub>10</sub>. (f) Arrhenius analysis of horizontal shift factors for all CAN B<sub>10</sub> samples. Filled circles are from frequency sweep data and empty circles from stress relaxation; each color is a single sample. Dashed line is line of best fit.  $T_{ref} = 175$  °C for all analyses.



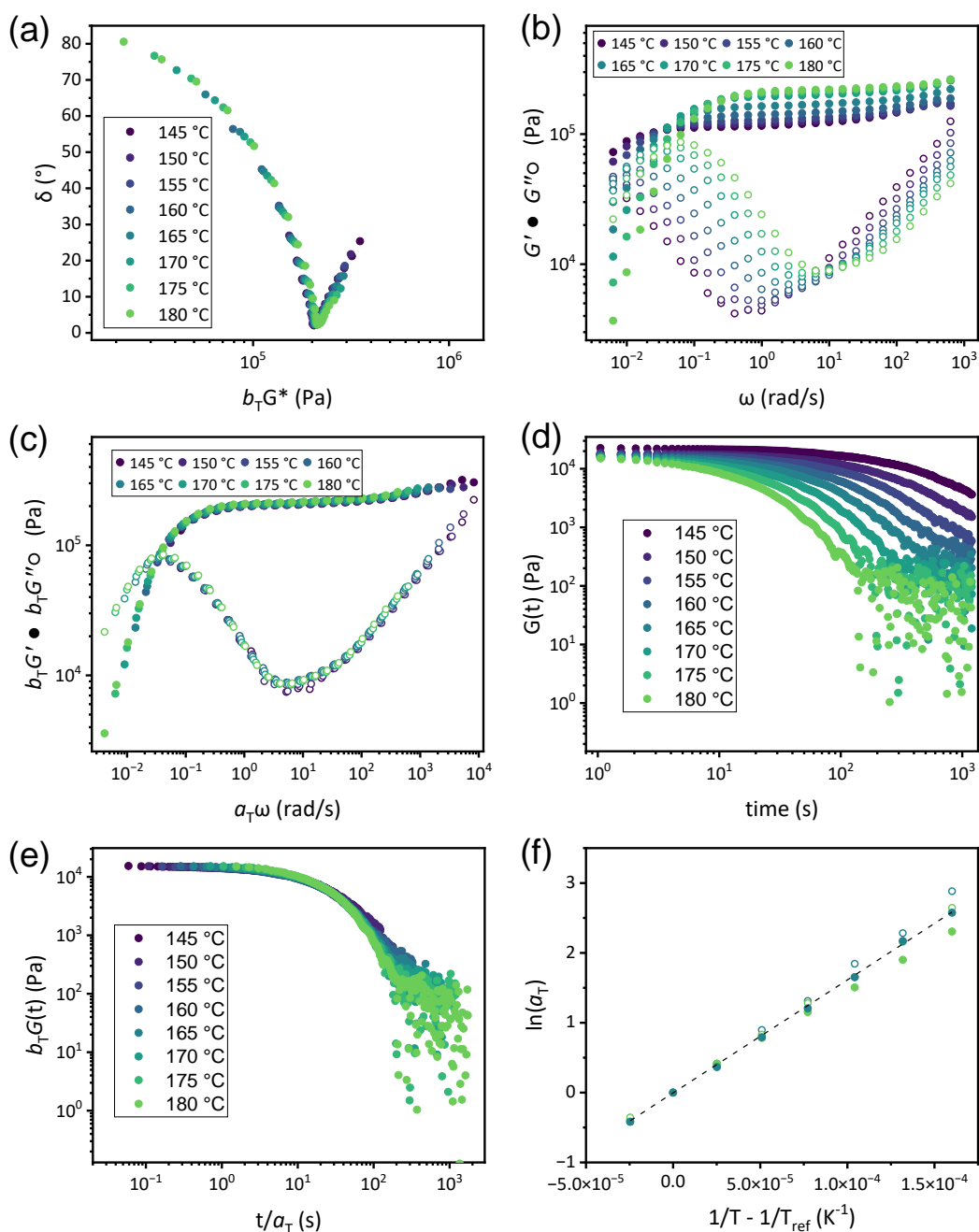


**Figure S49.** (a) Reduced van Gurp-Palmen plot of a sample of CAN C<sub>10</sub>. (b) Unshifted frequency sweep data of a sample of CAN C<sub>10</sub>. (c) Master curve of frequency sweep data constructed via TTS of a sample of CAN C<sub>10</sub>. (d) Unshifted stress relaxation data of a sample of CAN C<sub>10</sub>. (e) Master curve of stress relaxation constructed from TTS of a sample of CAN C<sub>10</sub>. (f) Arrhenius analysis of horizontal shift factors for all CAN C<sub>10</sub> samples. Filled circles are from frequency sweep data and empty circles from stress relaxation; each color is a single sample. Dashed line is line of best fit.  $T_{ref} = 175$  °C for all analyses.

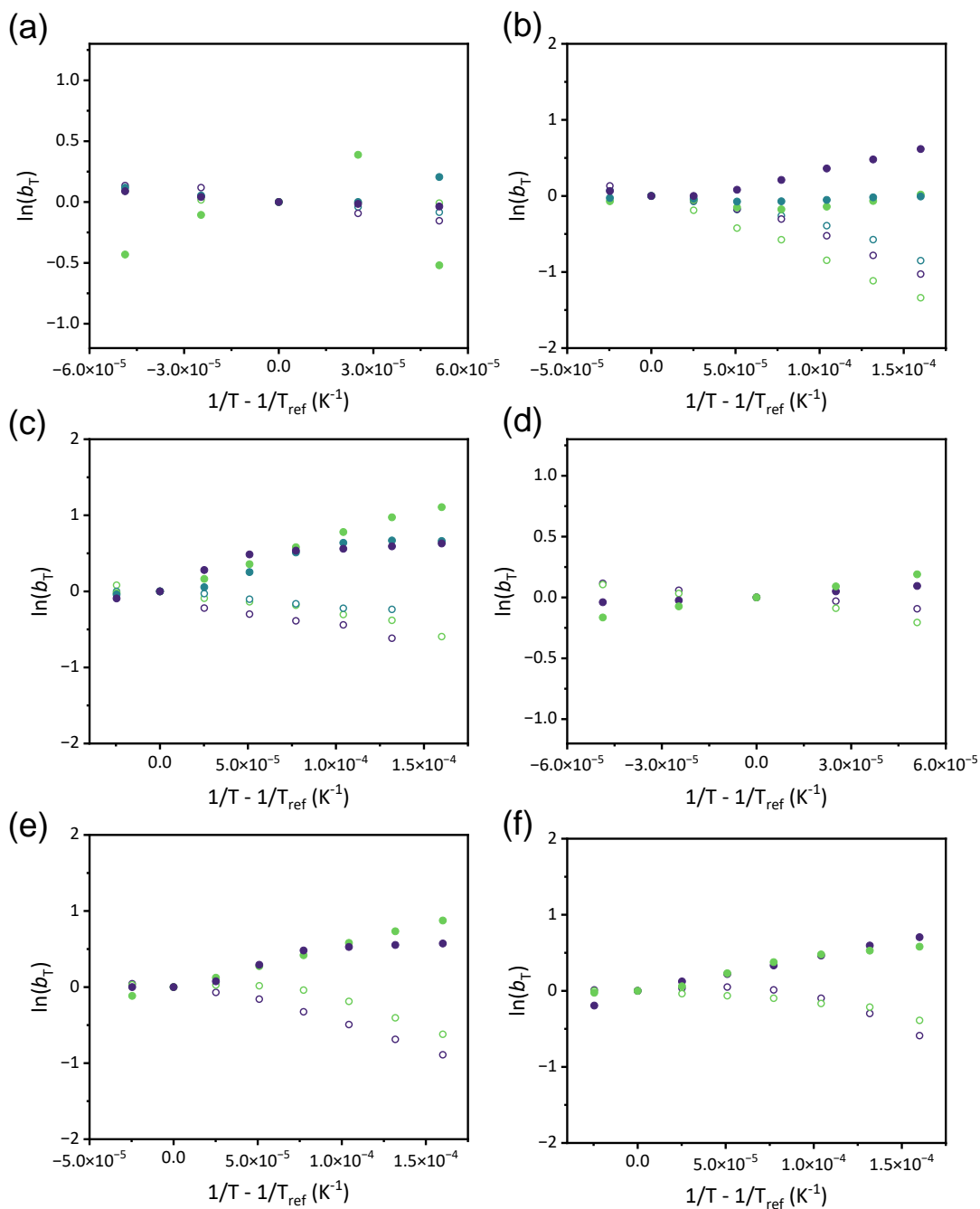


**Figure S50.** Arrhenius analysis of vertical shift factors for CAN samples. (a) CAN A<sub>5</sub>; (b) CAN B<sub>5</sub>; (c) CAN C<sub>5</sub>; (d) CAN A<sub>10</sub>; (e) CAN B<sub>10</sub>; (f) CAN C<sub>10</sub>. Filled circles are from frequency sweep data and empty circles from stress relaxation; each color is a single sample.  $T_{ref} = 175$  °C for all analyses.

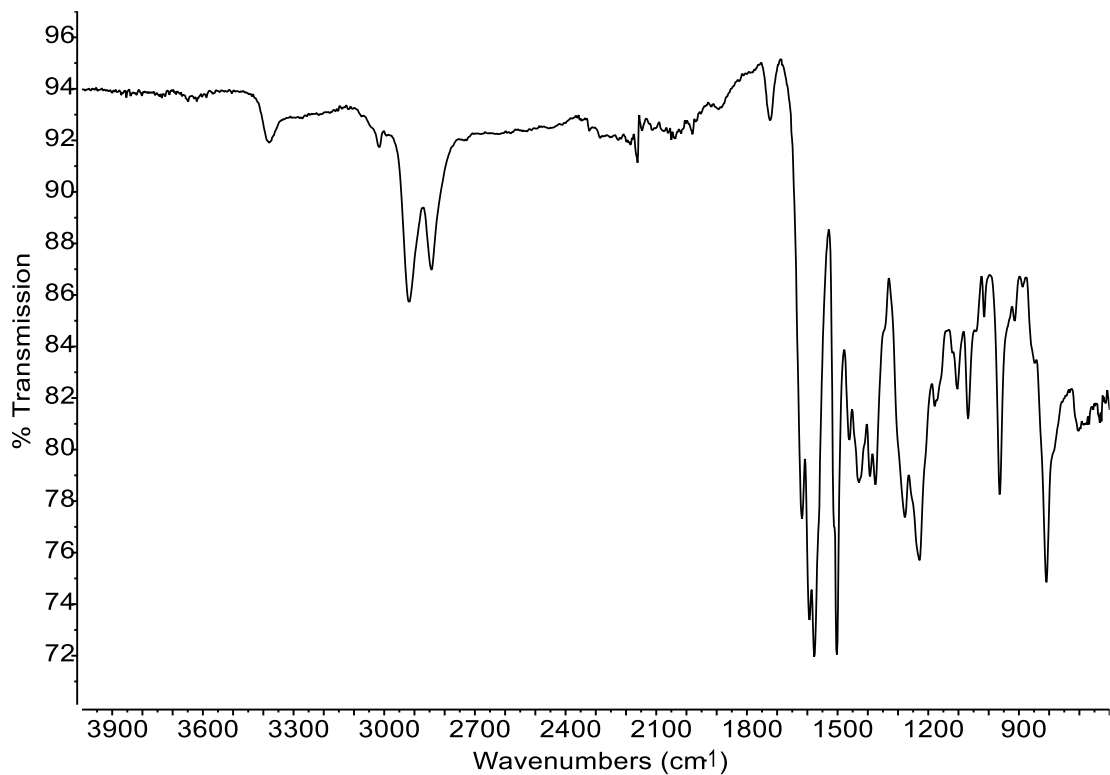
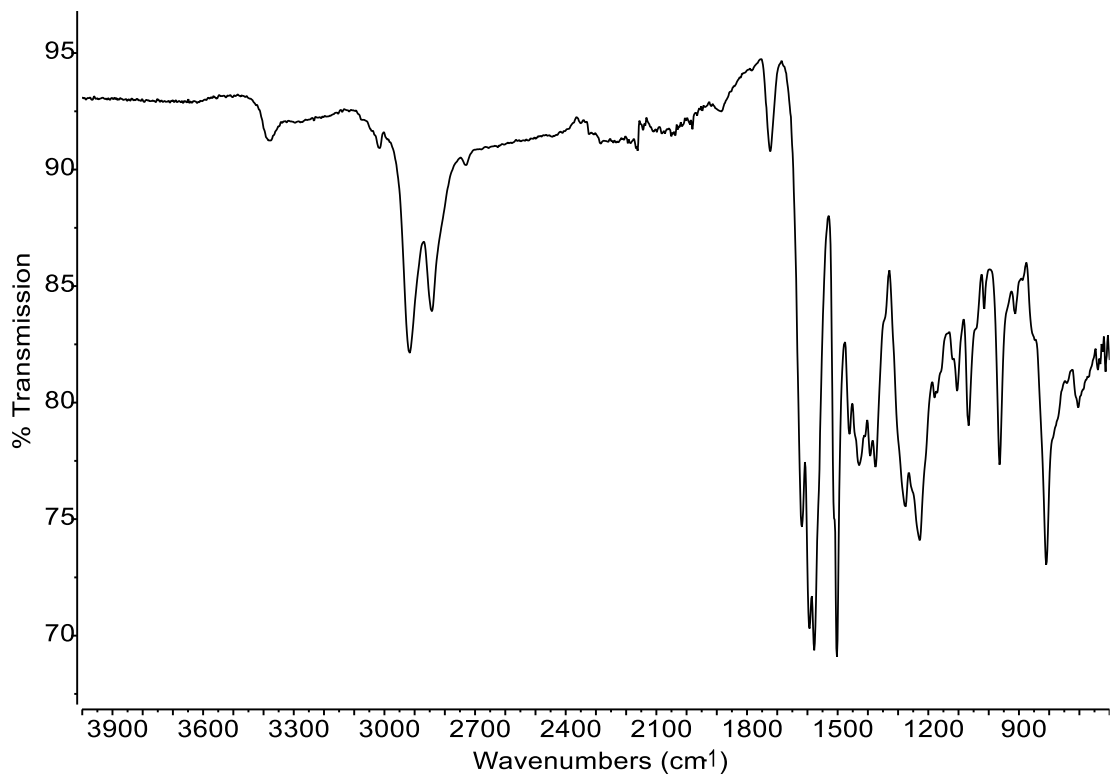


**Figure S51.** ATR FT-IR spectra of a sample of CAN A<sub>5</sub> before (top) and after (bottom) rheological analysis.

**Discussion of the sticky Rouse model for unentangled CANs.** The terminal relaxation time ( $\tau_{term}$ ) in this model is expressed as

$$\tau_{term} = \tau_{xl} N_{xl}^2$$

where  $\tau_{xl}$  is the crosslink lifetime and  $N_{xl}$  is the number of crosslinks per chain. While our systems do not achieve terminal relaxation in the experimental conditions, the longest relaxation times we observe (i.e.,  $\tau^*$ ) still follow this trend.  $\tau_{xl}$  can be further described as

$$\tau_{xl} = \sigma \tau_0 \exp\left(\frac{E_a^{sm}}{RT}\right)$$

where  $\sigma$  describes the mobility of the exchanging functional group,  $\tau_0$  is the Rouse segmental relaxation time, and  $E_a^{sm}$  is the activation energy of the crosslink exchange reaction. Thus, if  $\sigma$  is relatively constant under the experimental conditions, the temperature dependence of  $\tau_{xl}$  (i.e., the flow  $E_a$  measured by rheometry) will only be dependent on  $E_a^{sm}$  and  $\tau_0$ . For additional discussion and comparison to other models of CAN dynamics, see main text refs. 52 and 54.